

Anatomically inspired scaffold design enhances tissue regeneration in brain and spinal cord

by

Darice Yukfun Wong

A dissertation submitted in partial fulfillment
of the requirements for the degree of
Doctor of Philosophy
(Biomedical Engineering)
in The University of Michigan
2007

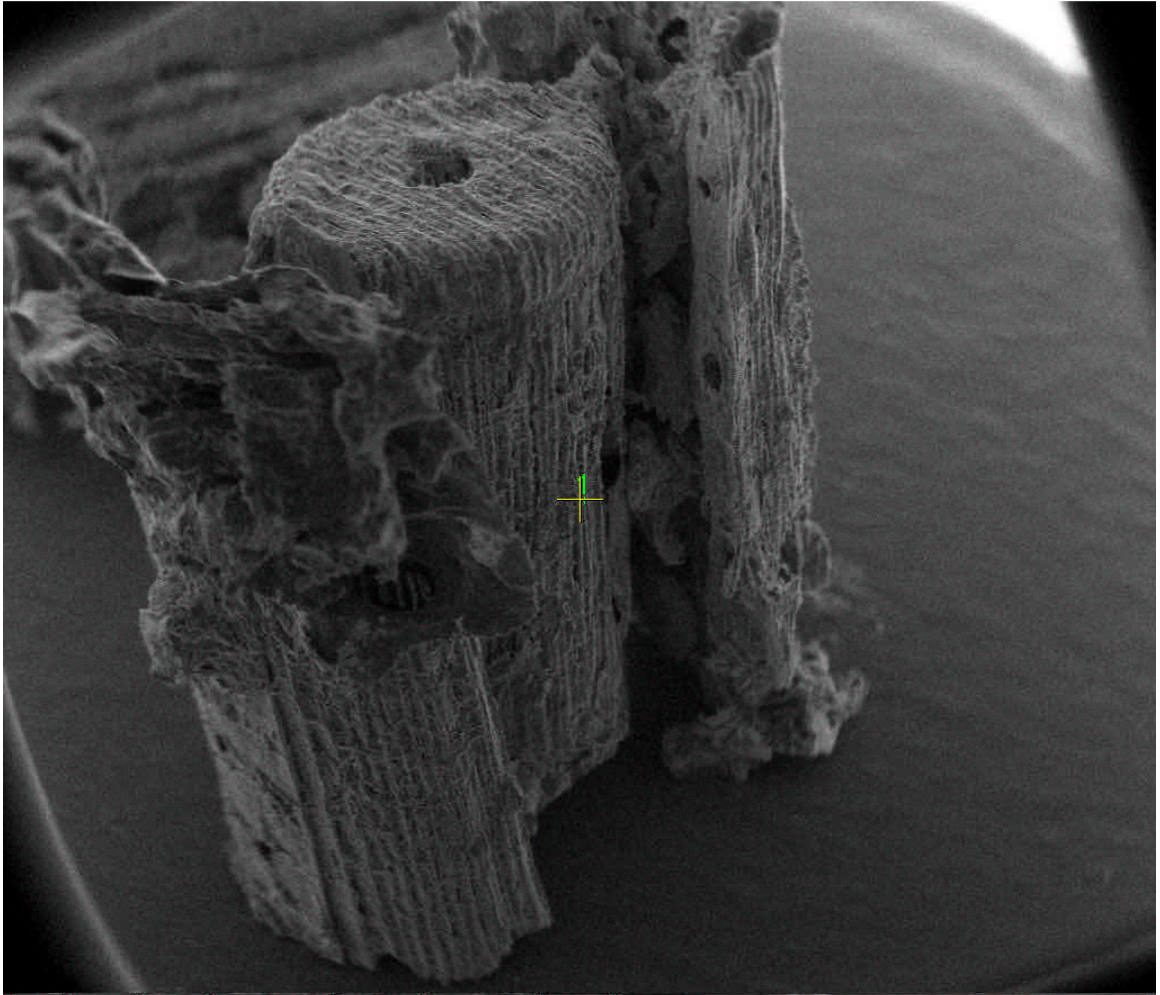
Doctoral Committee:

Professor Scott J. Hollister, Chair

Professor Paul H. Krebsbach

Assistant Professor Frank LaMarca

Professor Christopher A. Nosrat, University of Tennessee, Memphis



The “Tie-Fighter”

© Darice Yukfun Wong 2007
All Rights Reserved

To my parents Dr. and Mrs. K.C. and Nancy Wong, who always encouraged me to go to graduate school and never have a boyfriend, and my husband Jason Kutch who was my boyfriend and graduate school companion. Also to Dr. Shen, whose life and death inspired me to study the biomedical sciences.

ACKNOWLEDGEMENTS

I would like to thank my advisors Scott Hollister and Paul Krebsbach for both their guidance and the freedom they afforded me in my research. It has been a wonderful and expansive journey, and I'm sure I've learned more than I realize.

I am grateful for the wonderful support of my former and current labmates in the Hollister lab and Krebsbach lab. In particular for their advice, help, camaraderie, and friendship in this endeavor: thanks to Juan Taboas, Rachel Maddox-Schek, Catherine Kuo, Chia-Ying Lin, Colleen Flanagan, Elly Liao, Eiji Saito, Jessica Kemppainen, Erin Moffitt, Alisha Diggs, Sarah Mantilla, Claire Jeong, Annie Mitsak, Huina Zhang, Heesuk Kang, Wilbur Tong, Pat Racenis, Shelley Long, Erica Scheller, Hwei-Wen Lee, Zhuo Wang, Jun-Hui Song, and Premjit Arpornmaeklong.

The Spine Lab under the direction of Frank LaMarca and Chia-Ying Lin has also been a wonderful source of support and I'd like to thank Frank and Chia-Ying for keeping an interest in my research while it diverged from their own. Several medical students and residents have come to help me with this project through the Spine Lab and without their efforts much of this dissertation could not have been possible. Deep thanks go to J.C. Leveque, Hunter Brumblay, and Alex Garnepudi for performing the spinal cord implant surgeries and animal care. Thanks also to Emily Brunner and Steve Gross for their UROP summers trying to get things to work, it was not in vain.

I'd like to thank my other committee member Chris Nosrat and his colleague

Kristina Holmberg, particularly for the advisory roles they played in this non-neuroscientist's research on the central nervous system. I could not have learned so much without their help, enthusiasm and encouragement.

There is a body of work apart from this dissertation which served equally in my education, and for that I must thank Sue O'Shea, Theresa Gratsch, and Andrew Fribley. At a time of uncertainty and frustration they helped me resolve my problems and put it behind me.

Administrative details and paperwork are never fun to deal with, but these people have made my life infinitely better: Liz Rodriguiz, Wanda Snyder, Maria Steele, Tonya Brown, Sandy Staneff, and Pat Schultz.

I'd like to thank two of my friends, Elly Liao and Christine Tse, for defending right before me. It's nice to have someone to compare notes with and see that it can actually be done. They have been my guides through the details and make it seem almost easy. Thanks to Wilbur Tong for sharing lab space with me, listening to me complain, showing me his scuba pictures, losing the travel globe, finding it again, and helping me proof read my dissertation but not showing up to the defense. Thanks also to Colleen Flanagan for her friendship and support in and out of the lab, a tremendously talented person in every way, especially on a sail boat.

Thanks to my old friends, Neda and Jay, for reminding me there's another world out there that I should visit every so often, and not just for weddings.

Lastly, I'd like to thank my husband, Jason Kutch, who gave up South Africa and then sunny southern California to go to graduate school with me. He has influenced everything I have done, and even set up the Latex program to format my dissertation. He works tirelessly both with me and for me. He is my best friend and forever school-mate. We will learn together for the rest of our lives.

TABLE OF CONTENTS

DEDICATION	ii
ACKNOWLEDGEMENTS	iii
LIST OF FIGURES	vii
CHAPTER	
I. Dissertation Overview	1
1.1 Background and Motivation: CHAPTER II Overview	1
1.2 Identifying PCL as suitable material for studying macro-architecture in CNS: CHAPTER III Overview	3
1.3 Designing and fabricating different architectures for CNS regeneration in rat cortex model: CHAPTER IV Overview	4
1.4 Designing and fabricating different architectures for spinal cord and testing in a rat spinal cord transection model: CHAPTER V Overview	5
1.5 Summary and Future Work: CHAPTER VI Overview	7
II. Background and Motivation	9
2.1 The nervous system: Disorders, injuries, and clinical treatments	9
2.1.1 History:	10
2.1.2 Obstacles to regeneration in the central nervous system:	11
2.1.3 Disorders and injuries:	14
2.1.4 Clinical treatments:	15
2.2 Past central nervous system repair strategies	17
2.2.1 Cell sources	17
2.2.2 Trophic factors and extracellular matrix proteins	20
2.2.3 Topographical cues and patterned substrates	22
2.2.4 Mechanical properties and neural cell behavior	24
2.3 Macro-scale architectural influences and potential uses	25
2.3.1 Scaffolds for brain injury repair	27
2.3.2 Scaffolds for spinal cord injury repair	28
2.3.3 Designed architectures in the central nervous system	33
III. PCL and PLGA degradable polymer sponges attenuate glial scarring and lesion growth in traumatic brain injury	41
3.1 Overview	41
3.2 Introduction	42
3.3 Methods	45
3.4 Results	49
3.5 Discussion	55

3.6	Conclusions	63
IV.	Interconnected channels and aligned microgrooves promote cerebral cortex regeneration	65
4.1	Overview	65
4.2	Introduction	66
4.3	Methods	69
4.4	Results	74
4.5	Discussion	81
4.6	Conclusions	84
V.	Open-path architectures promote nerve fiber regeneration and decrease secondary damage in spinal cord injury	86
5.1	Overview	86
5.2	Introduction	87
5.3	Methods	90
5.4	Results	93
5.5	Discussion	99
5.6	Conclusions	103
VI.	Summary and future work	104
6.1	Summary	104
6.2	Related research for future work	106
6.2.1	Modifications to fabrication process	107
6.2.2	Modifications to design	108
6.2.3	Surface modifications and delivered components	110
6.3	Prospectus for future work	119
APPENDIX	122
BIBLIOGRAPHY	130

LIST OF FIGURES

Figure

2.1	A schematic diagram of rat and human brain in coronal cross-section with cerebral cortex organization highlighted.	36
2.2	A schematic diagram of the spinal cord.	39
3.1	H&E stained sections of PCL and PLGA polymer constructs in brain cavities. . . .	48
3.2	SEM micrographs of PCL surfaces cast with acetone and chloroform as solvents. . .	50
3.3	Quantitative data comparing control, PCL, and PLGA from image analysis.	52
3.4	OX-42 immunohistochemistry for control, PCL, and PLGA.	56
3.5	GFAP immunohistochemistry for control, PCL, and PLGA.	57
3.6	Representative immunofluorescent images identifying neural cells in PCL and PLGA. 58	
4.1	Schematic drawings and fabrication details of (a) Cylinder, (b) Channel, and (c) Orthogonal design scaffolds.	71
4.2	Gross images of implant groups and diagramed quantitative methods.	72
4.3	Representative and corresponding sections for cylinder, channel, and orthogonal scaffolds H&E stained and labeled for GFAP for 4 weeks implantation.	76
4.4	Representative and corresponding sections for cylinder, channel, and orthogonal scaffolds H&E stained and labeled for GFAP for 8 weeks implantation.	77
4.5	Nestin and Tuj-1 labeled sections of cylinder, channel, and orthogonal scaffolds from 8 week time points.	79
4.6	Quantification of defect widths, total cellular ingrowth, parenchymal inflammation, and astrocytic infiltration of cylinder, channel, and orthogonal scaffolds.	80
5.1	Design and fabrication of macro-architectures for spinal cord implants.	91
5.2	Control defect, no scaffold implant, at 1 and 3 months, sagittal sections H&E stained and immunolabeled.	94
5.3	Cylinder implant at 1 and 3 months, sagittal sections H&E stained and immunolabeled for GFAP and Tuj-1.	96

5.4	Tube and channel implants at 1 and 3 months H&E stained and immunolabeled for GFAP and Tuj-1.	97
5.5	Open-path designs with and without core, sagittal sections stained and immunolabeled.	98
5.6	Defect lengths and illustrations of possible interactions.	100
6.1	Micro-CT scan of a PCL scaffold made by a freeze-drying method in a wax mold. .	107
6.2	Standard curves for bovine serum albumin (BSA), fibronectin (FN), and laminin (LN) adsorption onto PCL films.	111
6.3	Total protein adsorption and concentration per surface area onto PCL films for bovine serum albumin (BSA), fibronectin (FN), and laminin (LN).	112
6.4	Two separate populations of BMSC seeded selectively into separate locations in a macro-designed PCL scaffold.	113
6.5	RT-PCR bands for nestin and musashi mRNA expression in BMSC cultured in monolayer and in 3-D scaffolds with and without serum replacement medium. . .	116
6.6	Expression of nestin protein by BMSC in monolayer was confirmed by immunocytochemistry.	117
6.7	Expression of musashi protein in monolayer was confirmed by immunocytochemistry.	117
6.8	Expression of Tuj-1 protein after SR medium treatment in monolayer was found in small proportions by immunocytochemistry.	118

CHAPTER I

Dissertation Overview

1.1 Background and Motivation: CHAPTER II Overview

Because traumatic damage to the central nervous system (CNS) (in particular, brain and spinal cord) has no clinical cure, various regenerative and reparative strategies are under scientific investigation. The current literature in CNS regeneration is focused largely on the following components: biomaterials, neurotrophic factors, and cells. Though there is a consensus that the ultimate treatment will consist of a combination of these components, the effects of each individual component should be understood to enable practical testing of the most promising combinations.

In the category of biomaterials, recent research has investigated the ability of the materials to deliver the other two components, neurotrophic factors and cells, to central nervous system defects (Schwab et al., 2006; Schmidt and Leach, 2003). Architectures and topographies of these biomaterials have been of interest mostly on the cellular scale, or micro-scale, for influencing cell behavior based on contact guidance (Curtis and Wilkinson, 1997).

The macro-scale architectures are not as diversely investigated as the micro-scale topography. Single and multi-channeled guidance tubes are the most commonly used macro-architectures for spinal cord injury (Nomura et al., 2006). Treatments

for traumatic brain injury have only used hydrogels and sponges with no macro-architecture at all (Schouten et al., 2004; Hou et al., 2005; Tian et al., 2005a). The focus of each study has been the neurotrophic factors or cells used in conjunction with the biomaterial, or preliminary study of a single biomaterial construct for later pairing with neurotrophic factors or cells. There have been no rigorous comparative studies of macro-architectures of biomaterials in brain or spinal cord defects.

There is some evidence that macro-architecture could influence nervous tissue regeneration. In other tissues such as bone and cartilage, interconnected pores and open macro-architectural features improve tissue ingrowth (Li et al., 2007; Malda et al., 2005; Otsuki et al., 2006), aspects which have not been studied in brain tissue but may be important. Also in a spinal cord transection model, a 4-channeled guidance tube improves neuronal regeneration and functional recovery over a single channeled tube, presumably due to increased surface area (Tsai et al., 2006).

The influence of macro-architecture is suggested in these studies, but the extent of influence is unknown. If the architecture of a scaffold on its own is able to improve the regeneration potential in the CNS, its use would enhance the effects of other combination treatments like neurotrophic factors or implanted cells. Use of effective architectures could also potentially decrease any dosing requirements for expensive or limited treatments such as recombinant proteins or autologous cells. It is thus hypothesized that creating a more diverse set of macro-architectures based on known anatomical characteristics of the tissue would improve the regenerative capacity of the CNS.

1.2 Identifying PCL as suitable material for studying macro-architecture in CNS: CHAPTER III Overview

Rationale: The brain and spinal cord are very different in structure and organization though they contain similar cell types. Therefore, reactions to scaffolds and appropriate architectures would likely be different. Before testing the main hypothesis in the two model systems, brain and spinal cord, a model material was chosen. Two degradable materials were chosen to fit the following criteria: 1) strength enough to maintain a macro-architecture yet elastic enough to be used in soft tissue, 2) the ability to accommodate controlled drug release or surface modification in future applications 3) non-immunogenic and 4) do not completely degrade within a few weeks *in vivo*. A rat cerebral cortex defect model similar to other published research was chosen for ease of study and comparison (Tian et al., 2005a). The defect is relatively superficial in the brain and does not cause any functional loss, thus surgery remains simple and husbandry duties remain at a minimum. Cortical loss is also typical in traumatic brain injury.

Summary: Poly(ϵ -caprolacton) (PCL) and poly(lactic-co-glycolic acid) (PLGA) were chosen to be examined in brain for biocompatibility as porous scaffolds. Both were found to suppress defect growth, a result of secondary cell death, over the control containing no material. Additionally, the PCL implant contained fewer MHC-II positive activated macrophages, but activated more CD11b positive resident microglia at an earlier stage than PLGA, an indication that the cellular response was less inflammatory and more neuroprotective in PCL than PLGA. The remaining studies thus were performed using salt-leached PCL as the base material.

1.3 Designing and fabricating different architectures for CNS regeneration in rat cortex model: CHAPTER IV Overview

Rationale: Macro-architectures have not been evaluated in scaffolds for brain tissue regeneration. In the cerebral cortex, neurons are organized into six generally transverse layers, parallel to the surface of the cortex. Their axons project vertically, perpendicular to the surface, in columns connecting the cortex with deeper regions of the brain. Information is therefore relayed between neurons in this vertical columnar organization in groups spanning 300-600 μ wide. Macro-architectures were therefore selected for study that incorporated these organizational directions and layers into the guidance channels. The same cortical defect model was used here as in the first polymer comparison study.

Summary: To test the hypothesis in the brain, interconnecting and isolated channels and microgrooves were incorporated into a porous cylindrical scaffold with the following combinations and implanted into a rat cerebral cortex defect extending inward 3 mm from the surface: 1) no channels or microgrooves, 2) 5 channels and microgrooves along all walls oriented vertically in the brain, and 3) 5 channels oriented vertically in the brain interconnected by orthogonally intersecting channels parallel to the brain surface at 3 evenly distributed heights along the cylinder and transverse microgrooves parallel to the brain surface.

The results demonstrated that, 8 weeks post-implantation, interconnected channels increased inward migration of glial cells (GFAP astrocytic marker), as well as organization of neuronal (Tuj-1 axonal marker) and progenitor (nestin filament marker) cell types from the lateral parenchyma over porous scaffolds with non-interconnecting channels and porous scaffolds with no channels at all. There was very little migration of host cells from the center of the brain toward the surface. The results also showed

that microgrooves increased organization and axonal projection along their direction of orientation *in vivo*. Also larger pore sizes (100-250 μm versus $< 50 \mu\text{m}$) increased total cellular ingrowth. Thus, in the rat cerebral cortex, regeneration into a porous scaffold can be enhanced with interconnecting channels and microgrooves oriented in the direction of desired migration.

1.4 Designing and fabricating different architectures for spinal cord and testing in a rat spinal cord transection model: CHAPTER V Overview

Rationale: Scaffold architectures in recent literature fall into three categories: porous cylinder, single or multi-channeled tubes, and microfilament bundles. Though their overall shape is influenced by the cylindrical shape of the spinal cord, their architectures are not directly influenced by the locations of the white matter (circumferential) and gray matter (central). In addition, they all fill the defect cavity to its lateral perimeters. Therefore designs were created to determine the benefit of medial physical support for white matter tracts and the necessity of complete circumferential presence.

Summary: To test the hypothesis in the spinal cord, porous scaffolds were made in a variety of architectures: cylinder, tube, 5-channel, and two novel open-path designs. These new designs were influenced by 1) the circumferential location of white matter tracts, 2) the central core location of gray matter, 3) the cylindrical bony enclosure provided by the spinal canal, and 4) the central canal, the conduit for cerebrospinal fluid (CSF). There are rounded top and bottom shells attached with fins to a central cylindrical core with a small channel through the middle (Figure 5.1). The core is designed to support the white matter tracts from the inside to prevent the typical cavitation that occurs when the gray matter degenerates. The core would also provide a medium for cell seeding to support gray matter regeneration

in the future. A small channel through the center aims to reduce impedance of CSF flow. The top and bottom shells are designed to provide structural support to the central core, holding the core up in the middle, while also keeping scar and muscle tissue above the defect from entering and inhibiting regeneration of the white matter. The shells also provide added surfaces for white matter growth. The second novel design is a control for the central core in that there are two shells but only one fin connecting the shells and no central core. Thus it is a tube with discontinuous walls. The discontinuous outer shells make the scaffold slightly narrower than the cylinder, tube, and channel designs, facilitating their implantation without requiring excessive removal of the spinal processes.

Implantation into a complete spinal cord transection at T8 resulted in fibrous tissue encapsulation of the cylinder. Oriented fibrous tissue growth through both the channels and the tube with no connecting neural tissue was observed through GFAP and Tuj-1 immunohistochemistry. A high degree of secondary damage in the cylinder, tube, and channel designs was observed from the doubling of the defect length from the original size. The open-path designs were able to maintain the defect length in the gray matter and also support robust nerve fiber growth around the outer shells, bridging the defect site. Additionally the open-path design with a central core cylinder was able to support axonal growth straddling the shells and within the core. The improved integration of neural tissue and suppression of secondary damage in the gray matter demonstrated that not only does scaffold architecture have an effect on spinal cord regeneration, but a complete entubulation of the site and enclosure of the defect site by guidance channels is not necessary to provide an environment conducive to regeneration.

1.5 Summary and Future Work: CHAPTER VI Overview

In the cerebral cortex, lateral migration of host cells is increased by lateral interconnecting channels, but vertical migration is not enhanced by vertical channels alone. Vertical organization of axonal transmission is eclipsed by the need to first repopulate the defect cavity with cells from the lateral laminae, but microgrooves and vertical channels could improve vertical organization of axonal projections in the cavity once it is repopulated. In different animal models or different regions of the brain, modifications can be made to the overall size, shape, and orientation while maintaining the principle of interconnected channels and directed microgrooves.

In a thoracic spinal cord transection, entubulation is not necessary particularly when the spine still partially provides a natural enclosure. Medial support of regenerating white matter tracts from the central core and outer shells prevents secondary damage in the centralized gray matter, possibly because of neuroprotective effects of regenerating nerve fibers and rostral nerve roots which are able to enter and bridge the open defect site. More clinically applicable injury models in the spinal cord, such as contusion or hemisection, could be accommodated with variations based on the principles of anatomical structural support found here.

These are the first experiments using scaffolds made by indirect SFM techniques to have designed architectures in CNS regeneration. They show that different macro-scale architectures can affect tissue regeneration in the CNS, while micro-scale topography is confirmed to affect cellular behavior *in vivo*. The contribution of this work is to bring attention to the wide range of architectural possibilities for biomaterials in CNS regeneration. In addition to the delivery of neurotrophic factors and cells, appropriately designed biomaterials can enhance the regenerative potential of

a defect site.

Because these architectures are created from a mold process, the material and the method of generating micro-pores may be changed. Variation on these designed architectures can be extensive. Each of the designs for these CNS injury models can and should be combined with other tools for regeneration: neurotrophic factors, cells, or extracellular matrix molecules. A prospectus on these combinations is included.

CHAPTER II

Background and Motivation

2.1 The nervous system: Disorders, injuries, and clinical treatments

The central nervous system (CNS) is comprised of the brain, and spinal cord. Within this system is a control network for the many functions of the body. Humans are most physically aware of the sensory and motor systems, that are controlled by different regions within the CNS. On a cellular level, each of these regions and systems is made up of specific cell types. Neurons are largely responsible for the relay of signals, action potentials, throughout the nervous system and physically carry the information, most notably via their axons. The other cells in the CNS are glial cells (astrocytes, oligodendrocytes, ependymal cells, and microglia the immune cells of the brain) which vastly outnumber the neurons and are responsible for myelinating the neurons and a host of other versatile functions. (For detailed information see Principles of Neural Science Chapter 1, (Kandel et al., 2000)) The complexity of the nervous system drives prolific research from the neuroscience community in an attempt to understand all of its astounding capabilities and occasionally its devastating shortcomings.

2.1.1 History:

The earliest studies of nerve regeneration date back to 1776 when William Cruikshank was studying the vagus nerves of dogs (Ochs, 1977). It was known then that simultaneous bilateral vagus nerve transection resulted in death after a few days. In a series of vagus nerve transection experiments varying the time between transections and also single vagus nerve transections, Cruikshank observed the breathing, digestive behaviors, and time to death, followed by microscopic analysis of the dissected nerves, and identified tissue connecting the two cut ends in some animals with longer survival times. This connecting tissue was identified by simple microscopic techniques to be similar to nerve tissue.

As the common occurrence of death became a problem in further study of peripheral nerve regeneration in the vagus nerve, the sciatic nerve became the favored location for nerve regeneration studies with other scientists of the time, particularly in cats, rabbits, and frogs (Ochs, 1977). By the 1800s it was generally accepted that peripheral nerves could regenerate. Debate and research concerned only the mechanism.

However, regeneration in the CNS, particularly in humans, was widely believed to be impossible. Salamanders and newts, lower vertebrates, can regenerate spinal cords readily, but until the mid 1900s there was a strong belief within the scientific community that regeneration in higher vertebrates was impossible, and that research to that effect was a waste of time (Windle, 1981). Though axons in injured spinal cord, cerebral cortex, and optic nerve were described to undergo a period of abortive sprouting before degeneration (Ramón y Cajal et al., 1991), it was concluded that axons in the CNS were unable to regenerate beyond the abortive sprouting phase because of the lack of Schwann cells, which seemed to improve the sprouting of axons

in peripheral nerve (Ramón y Cajal et al., 1991).

The first suggestive evidence of regeneration in the spinal cord of higher vertebrates was presented in 1940 with regard to immature rats which, after implantation of sciatic nerve grafts between severed spinal cord stumps, demonstrated some anatomical, physiological and behavioral recovery in some of their animals (Sugar and Gerard, 1940). This evidence was refuted by most scholars and not taken up again until 1950 while studying central regulation of body temperature in cats and dogs, a study which required transection of nerves at different levels, including the spinal cord. After some period of time it was noticed that pain was sensed by dogs upon bladder expression by the researchers (Windle and Chambers, 1951).

The National Paraplegia Foundation sought to increase the visibility of this type of research and funding and support from governments by holding conferences (now the National Spinal Cord Injury Foundation) which had rehabilitation medicine as a strong alternative to regeneration research (Windle, 1981). It was then regarded that without grafting or other techniques, spontaneous and complete regeneration of severed axons could not occur in mammalian CNS. With the advancement of analytical techniques and the increased interest in this research topic there now exist several promising pathways of investigation for CNS regeneration (Windle, 1981; Batchelor and Howells, 2003; Schwab et al., 2006).

2.1.2 Obstacles to regeneration in the central nervous system:

With the advancement of knowledge, it still remains that traumatic injuries in the CNS very rarely regenerate compared to injuries in the peripheral nervous system (PNS). Understanding and overcoming the large obstacles to regeneration in this area are the motivations of basic scientists and engineers alike, and have motivated the course of this dissertation.

The PNS is made up mostly of axons extending from neurons in the spinal cord, along with myelinating Schwann cells. When the PNS is injured Wallerian degeneration occurs (Rosenblueth and Dempsey, 1939), where severed axons die back and nerve function and conductance is lost. The myelin sheath can be left intact even after the axon has degenerated *in vivo* (Heath, 1982; Kidd and Heath, 1988a; Kidd and Heath, 1988b; Kidd and Heath, 1991). This remaining natural channel is sometimes able to guide axonal regeneration in the PNS with the help of neurotrophic factors (Frostick et al., 1998), though complete functional recovery to pre-injury levels remains unrealized.

Regeneration in the CNS is much more difficult. The differences between the PNS and CNS reveal possible reasons for their difference in regenerative potential. Schwann cells in the PNS normally myelinate axons but upon injury they can also act as scavengers of cellular debris. Schwann cells, along with macrophages which are activated by the complement cascade after injury, can clear an injury site of regenerative inhibitory debris within several weeks (Hughes et al., 2002). In the CNS oligodendrocytes do not clear debris during Wallerian degenerating, leaving macrophages entering from circulation with a more delayed time course than in the PNS (Hughes et al., 2002) to do this work. Instead, oligodendrocytes become reactive after injury, upregulating the expression of transmembrane semaphorin Sema4D/CD100 and versican, both inhibitory molecules to axonal regeneration. It was earlier thought that oligodendrocytes were passive during injury, and inhibitory molecules acted by virtue of being released into the injury environment from physical damage. However the active role of oligodendrocytes in axonal inhibition is now under investigation (Schwab et al., 2005).

The cellular debris from the primary injury contains myelin inhibitory molecules

such as Nogo-A and myelin associated glycoprotein (MAG). In normal tissue they are present in myelin to help keep axons aligned in myelin sheaths, but released at random into an injury site they also prevent axonal growth. Axons in the spinal cord undergo Wallerian degeneration in the first 30 minutes of injury but will also attempt to regenerate vigorously in the initial 6 to 24 hours after degenerating (Kerschensteiner et al., 2005). This type of regeneration was known to exist very early and termed abortive sprouting (Ramón y Cajal et al., 1991). Inhibitory signals from extracellular matrix proteins like chondroitin sulfate proteoglycans (CSPG) produced by proliferating activated astrocytes after injury (McKeon et al., 1991) and myelin inhibitory molecules released from myelin and oligodendrocytes after physical disruption eventually overwhelm these axonal growth instincts and prevent any recovery (Busch and Silver, 2007).

The inflammatory reaction, infiltration of macrophages, and scar formation are much higher in spinal cord than brain (Trivedi et al., 2006), but follow a general progression. Neutrophils are the first invading inflammatory cells, within hours. They phagocytose cellular debris and attract macrophages to do the same. However, neutrophils also release toxins and free radicals responsible for secondary tissue damage, while macrophages, upon digestion of myelin debris, also store and provide cholesterol for use in re-myelination. Microglia, the resident inflammatory cells of the nervous system, have many conflicting functions. Upon activation from injury, they can remove myelin debris, promote neurite growth, decrease astrocyte proliferation, and promote neuronal survival. They can also release free radicals and molecules which damage tissue and inhibit regeneration (Trivedi et al., 2006).

Soon after the inflammatory cells are activated, astrocytes are activated, mainly by the microglia. Astrocytes, microglia, and fibroblasts begin to proliferate and ac-

cumulate at the injury site, depositing extracellular matrix to seal up the wound and protect other regions from further damage, but also blocking regeneration (Schwab et al., 2006; Maier and Schwab, 2006). This accumulation of cells and ECM is called the glial scar, which particularly contains CSPG, produced by reactive astrocytes, a molecule which inhibits axonal regeneration (Busch and Silver, 2007; Hermanns et al., 2001). Though there are many obstacles to regeneration in the CNS, collateral sprouting and re-routing of connections through spared tracts does occur, resulting in spontaneous recovery of some function in a small number of cases (Kaegi et al., 2002; Kerschensteiner, 2007). As the scientific community increases its understanding of the CNS and its cellular and molecular mechanisms of injury and repair the information will be of critical importance to the development of clinical treatments and eventually cures.

2.1.3 Disorders and injuries:

There are a number of diseases which can cause varying degrees of damage to the CNS. Neurodegenerative diseases such as amyotrophic lateral sclerosis (ALS) and multiple sclerosis are demyelinating diseases where myelinating cells of the CNS are lost (De Carvalho et al., 2005; Miller, 2001). The causes are not understood but patients lose motor control. Parkinsons disease (PD), on the other hand, results from a loss of dopaminergic neurons and in many cases a larger parenchymal mass loss (Singh et al., 2007). The most noticeable symptom of PD is tremor. Alzheimers disease (AD) is marked by an abundance of neurofibrillary tangles and senile plaques in the brain followed by loss of cholinergic neurons mainly in the basal forebrain, and causes dementia (Jellinger, 2006).

Other insults to the CNS can result from an ischemic stroke, which deprives the brain of oxygen and causes cell death in the brain, or traumatic injuries to either

the brain or the spinal cord, which can cause a number of disabilities depending on the location of injury. There are no cures for CNS injuries or diseases. Currently, treatments are largely palliative.

2.1.4 Clinical treatments:

The disorders and injuries of the CNS are not only incurable, but lack adequate long-term treatments. The devastating and seemingly hopeless prognoses of these conditions is the motivation for tissue engineering research in the CNS, including this dissertation.

There are a number of pharmacological treatments for PD which essentially boost or replace dopamine in the brain, treating the symptoms but requiring increased dosing over time and eventually becoming inadequate. Surgical removal of brain tissue is a last resort due to complications and inefficient long-term control of symptoms. There is ongoing research on neuroprotective agents to prevent PD onset in high-risk individuals based on family history. Deep brain stimulation has made some interesting improvements for a specific subset of patients with PD and essential tremor (Singh et al., 2007) but all PD patients are still waiting for a cure. ALS and AD patients have a similar prognosis. Pharmacological treatments are unable to halt or reverse the disease progression.

Methylprednisolone has been administered for acute spinal cord injuries (SCI) in the first 8 hours of injury with mixed results for improving outcome and recovery by reducing secondary damage (Bracken et al., 1984; Bracken et al., 1990; Hall and Braugher, 1982). Two national clinical trials showed benefit in humans but the analytical methods have been challenged (Coleman et al., 2000; Hurlbert, 2000; Short et al., 2000; Tsutsumi et al., 2006; Tator, 2006; Leypold et al., 2007). Regardless of the methods for showing significance, its use does not repair the primary injury.

In the case of traumatic brain injuries (TBI), brain tissue undergoes a healing process which includes necrosis and/or apoptosis in regions originally undamaged (Williams et al., 2006; Raghupathi, 2004). A summarized comparison of the following injury models in rats, penetrating ballistic-like brain injury (PBBI), stab wound, lateral fluid percussion (LFP), cortical concussive injury (CCI), and middle cerebral artery occlusion (MCAO) (which approximates ischemic stroke), ((Williams et al., 2006) table 4) reveals that, due to physical trauma, there is generally some degree of hemorrhage. The greatest amount of hemorrhage occurs in PBBI. After the first day, when cells are disrupted and die of necrosis to form an initial injury, the lesion volume grows over the next 2-3 days as microvasculature in the perilesional area is disrupted and secondary cell death occurs, presumably due to local ischemic conditions. In MCAO, this secondary death can continue for several more days into a full week and reaches the largest lesion volume. Remote white matter injury, likely apoptotic, and macrophage infiltration occur in all these models anytime between the first few days and beyond two weeks. There are indications for surgical treatments to lessen potential secondary damage and to improve chances of survival after traumatic brain injuries. Clinical evidence suggests that surgical treatment such as craniotomy or evacuation of hematoma may improve outcomes in severe TBI that consist of parenchymal mass lesions and neurological dysfunction, particularly when defect volume is greater than 50 cm^3 , or 20 cm^3 when accompanied by a midline shift of at least 5 mm and/or cisternal compression on CT scan (Bullock et al., 2006). The most common reason for surgical intervention is to decrease intracranial pressure. With or without surgical treatment, secondary cell death after the first day continues to be a problem.

Though current treatments for CNS disease and injury can hope only to prevent

further damage or slow the disease progression, the field of tissue engineering aims to generate functional tissue and repair both primary and secondary damage. This is a significant proposal, as the difficulty is great. However it is also significant because the potential benefits are great and also a fundamental motivation for this body of work in CNS regeneration.

2.2 Past central nervous system repair strategies

The basic techniques behind tissue engineering involve some combination of bio-material scaffold, cells, and biologic cues such as trophic factors or substrate interactions (Langer and Vacanti, 1993). A recent review of experimental strategies specifically for spinal cord regeneration outlines five strategic categories: 1) neuroprotection for diminution of secondary damage by targeting the innate immune response of neutrophils, macrophages and the like 2) neurorestoration by remyelination and restoration of conduction through de-myelinated tracts 3) neuroregeneration by antagonisation of inhibitory factors like CSPG or Nogo-A or neuroregeneration by promoting axonal growth factors (neurotrophic factors) 4) axon guidance to specific sites of deafferentation and 5) neuroreconstruction with cell and tissue transplantation (Schwab et al., 2006). The following is a brief summary of current lines of scientific investigation in general CNS regeneration. Rather than by strategy, as they can vary for different regions of the CNS, they are categorized by tools for CNS repair to better highlight the focus of this dissertation and when appropriate are described in relation to this work.

2.2.1 Cell sources

Replacement cells from various sources are being investigated for treatment of diseases and injuries of the nervous system. Cell types in use fall primarily into one

of the following categories: Embryonic Stem Cells (ESC), Neural Stem Cells (NSC), Schwann Cells (SchC), Olfactory Ensheathing Cells (OEC), and Bone Marrow Stem Cells (BMSC) or Mesenchymal Stem Cells (MSC).

ESC from the blastocyst stage of the developing embryo can be differentiated into multiple neural lineages, including neural progenitor cells similar to NSC (Tabar and Studer, 2002). These cells, differentiated or not, have been investigated for use in treating many nervous system disorders including SCI (McDonald et al., 2004), PD (Ben-Hur et al., 2004), and ischemic brain injury (Takagi et al., 2005). Research pertaining to them is currently limited by regulatory restrictions on ESC derivation and poses a barrier within the US.

Aside from ESC derived neural progenitors, NSC can be isolated from the sub-ventricular zone of the hippocampus among other locations of the CNS (Doetsch et al., 1999; Temple and Alvarez-Buylla, 1999), and have also been shown to improve recovery in TBI (Shear et al., 2004), ischemic brain injury (Lee et al., 2007; Park et al., 2002), intracerebral hemorrhage (Lee et al., 2007), and SCI (Teng et al., 2002). The limitations for these cells lie in the difficulty of obtaining them from patients or donors.

SchC are myelinating cells of the Peripheral Nervous System (PNS). Their counterpart in the CNS is the oligodendrocyte. SCI has been most successfully treated so far with peripheral nerve grafts (Levi et al., 2002; Houle et al., 2006; Kuo et al., 2007; Dinh et al., 2007), whose SchC are able to re-myelinate CNS axons (Fukunaga et al., 2004). Because of this ability, SchC have been isolated from peripheral nerve biopsies (Salzer and Bunge, 1980; Morrissey et al., 1991) and cultured for implantation as a purified and expanded population in CNS repair (Martin et al., 1996; Pearse et al., 2004; Brook et al., 2001; Pinzon et al., 2001; Dinh et al., 2007;

Evans et al., 2002; Hurtado et al., 2006; Stokols et al., 2006). Though not a replacement for neurons of the CNS, they provide a beneficial environment which could enable the intrinsic neural progenitor cells to repopulate and regenerate the injury.

OEC are similar to SchC but can be isolated from the olfactory system, part of the CNS, via nasal biopsies in humans (Barnett et al., 2000; Feron et al., 2005). A component of a relatively regenerative region of the CNS, these glial cells are also able to re-myelinate regenerating axons in the CNS and improve functional recovery (Imaizumi et al., 1998; Ibrahim et al., 2006; Raisman, 2006; Barnett and Riddell, 2007).

BMSC or MSC are isolated from the bone marrow (Krebsbach et al., 1999). MSC are considered to be a purified stem cell population, while BMSC are considered a heterogeneous population from the bone marrow. Some studies show that these cells express neural markers and can take on similar morphologies after different treatments (Woodbury et al., 2000; Woodbury et al., 2002; Munoz-Elias et al., 2003; Munoz-Elias et al., 2003; Coyne et al., 2006; Keilhoff et al., 2006), but their ability to take on neural cell roles is controversial (Spyridonidis et al., 2005; Pauwelyn and Verfaillie, 2006). Though not often regarded as potential replacement cells, they have been shown to improve outcomes in CNS injuries (Nandoe et al., 2006) likely due to neuroprotective effects and secreted neurotrophic factors which alter the injured environment (Lu et al., 2007; Mahmood et al., 2003; Lu et al., 2002; Chen et al., 2002; Lu et al., 2001; Mahmood et al., 2001; Mahmood, 2002; Mahmood et al., 2002; Mahmood et al., 2004a; Mahmood et al., 2004b). They are the subject of several studies in CNS repair and should certainly be held as an important tool to investigate (Sykova et al., 2006b; Sykova et al., 2006a; Mahmood et al., 2005; Mahmood et al.,

2006; Mahmood et al., 2006b; Mahmood et al., 2006a).

Cells of any type have not been able to fully repair damaged CNS, and some also carry the caveat of potential tumor formation. They have a low survival rate when injected *in vivo* without any carrier and will most likely be used in combination with other tools for repair.

2.2.2 Trophic factors and extracellular matrix proteins

Neurotrophic factors such as nerve growth factor (NGF), brain-derived neurotrophic factor (BDNF), and neurotrophin-3 (NT-3) have long been known to strongly influence development of the CNS, and also to enhance different neuronal cell growth. Their influences on specific cell types are varied and not completely understood (Thoenen, 1991; Hyman et al., 1991). Their combined use in current investigations with other reparative tools, particularly cells, is an indication of how important they will be in the repair of damaged CNS (Houle and Ziegler, 1994; Bakshi et al., 2004; Piantino et al., 2006; Stokols and Tuszynski, 2006; Lu et al., 2007). However, the field of controlled release exists for the purpose of delivering small molecules such as neurotrophic factors over an extended period of time, longer than they would persist *in vivo* if they were just injected. These factors will likely not be effective without a material vehicle to carry them.

Extracellular matrix (ECM) proteins, peptides which mimic cell attachment domains in the ECM, and nano- or micro-structured materials which mimic the ECM architecture (Ellis-Behnke et al., 2006) are of interest in tissue engineering applications because of their encompassing influence on cell behavior (Larsen et al., 2006).

Fibronectin (FN) is one of the key proteins involved in cell adhesion and migration throughout the body. Its attachment mechanism, based in integrin binding, is found in a short peptide sequence of arginine, glycine, and aspartic acid (RGD)

(Pierschbacher and Ruoslahti, 1984). This peptide sequence has been used to functionalize numerous materials for biotechnology applications (Hersel et al., 2003). The FN protein itself is often adsorbed to materials to increase cell attachment, though the material properties affect its conformation when adsorbed (Lhoest et al., 1998; Keselowsky et al., 2003), which in turn affects its signaling capabilities with cells (Miller and Boettiger, 2003) and their strength of attachment and spreading (Iuliano et al., 1993). For the most part, FN is used in neural tissue applications to influence glial cells and indirectly influence neurons (Ahmed and Brown, 1999), though it may play a critical role in axonal extension from adult white matter (Tom et al., 2004).

Laminin (LN) is found in the basement membrane and has the most significant influence on neural cell alignment, neurite extension, and growth cone guidance (LuckenbillEdds, 1997; Kuhn et al., 1998). It is often included in studies for nerve regeneration and guidance, improving experimental outcomes *in vitro* (Recknor et al., 2004; Wen and Tresco, 2006; Attiah et al., 2003; Miller et al., 2001; Thompson and Buetner, 2001; Stabenfeldt et al., 2006) and *in vivo* (Hou et al., 2005). A peptide sequence responsible for the attachment and neurite extension properties of LN was also identified (Tashiro et al., 1989; Nomizu et al., 2000) and is being used in conjunction with a hydrogel to promote regeneration in the rat cerebrum (Cui et al., 2003). Though it seems that LN is the protein of choice for neurons, its peptide sequence does not support stem cell adhesion and differentiation *in vitro* (Saha et al., 2007).

Since cell signaling cascades and their control over cell phenotype and behavior can be influenced by the extracellular matrix and the cell-material interface, these cellular level material considerations will be essential to reparative strategies. Also because of their contact-dependent nature, a biomaterial scaffold will be integral in

their use for CNS regeneration.

2.2.3 Topographical cues and patterned substrates

The morphology of a surface, roughness or smoothness, on which cells are cultured has a great effect on the cellular and tissue interactions independent of the chemical characteristics of the material (Singhvi et al., 1994). Rough surfaces on implants have greater integration with bone, and less fibrous tissue encapsulation. Though the early information on these effects was not systematic with regard to sizes and shapes of roughness, there was a clear idea that different tissues and cell types reacted differently to different surface topographies. With the advancement of fabrication techniques, scientists are able to study the effects of controlled topographies of materials on cell growth and tissue interactions (Curtis and Wilkinson, 1997).

Topography can take on a large range of shapes and sizes, from pits and hills, holes and spikes, to stepwise or V-shaped linear or circular grooves. An early study of surface roughness compared to smoothness of the inner lumen of a guidance tube for peripheral nerve regeneration showed that random pored roughness on the order of $100\mu\text{m}$ resulted in a fibrous tissue filled channel with few regenerating myelinated axons compared with a smooth inner lumen. Though the smooth guidance tube contained greater numbers of myelinated axons, they were not attached to the inner lumen of the tube, while the rough lumen was well integrated with the infiltrating fibrous tissue (Aebischer et al., 1990). But by far the most interesting topographical feature for neural tissue repair is linear grooves for alignment and extension of neurites. Many variations on groove width, depth and plateau width have been generated and many cell types have been cultured *in vitro* to study their behavior.

Studies of chick embryo neurons *in vitro* revealed that with fixed groove widths at $8\mu\text{m}$ and ridge widths at $20\mu\text{m}$, a groove depth of $1\mu\text{m}$ elicited no alignment of

neurites, while at $2\mu\text{m}$ depth alignment was achieved, indicating a lower limit on feature size for neurite alignment (Clark et al., 1990). This was further supported when nanoscale features for groove width, depth, and ridge width were created and no alignment was achieved with neurites, while fibroblasts and endothelial cells were still sensitive to alignment cues (Clark et al., 1991). Nanoscale features are indeed very influential in osteoblast and osteoclast alignment (Ito, 1999), and meningeal cells along with their extracellular matrix (Manwaring et al., 2004) while for neurons it seems micron-scale features are more effective. Furthermore, an upper limit for neurite alignment seems to exist around the tens of microns, as grooved substrates coated with LN yielded higher percentages of aligned neurites *in vitro* with narrower ridges: $30\mu\text{m}$ being better than $200\mu\text{m}$ (Miller et al., 2002), and $10\mu\text{m}$ being better than $20\mu\text{m}$ (Goldner et al., 2006).

Indeed it seems that the constraint based on cell size and confinement to a continuous ridge has a great affect on neurite alignment. Particularly with increasing groove depth on single to tens of microns scale, the narrower the groove and ridge (while still above single micron scale), the more concentrated the focal adhesions are to the ridge, thus aligning the cytoskeleton with the grooved features (Ito, 1999). However, another study of dorsal root ganglion (DRG) neurons puts the upper limit for alignment at $10\mu\text{m}$ with a depth of 50-100nm (Tsuruma et al., 2006), a depth which was previously unable to affect chick embryo cerebellum neurons (Clark et al., 1991). It might indicate that different types of neurons have different behaviors due to topography. However, with this study the groove and ridge materials were glass and poly(ϵ -caprolactone) with a poly-lysine coating (Tsuruma et al., 2006). These two materials have the added possibility of affecting the poly-lysine adsorption properties and varying the effects of this cell adhesive molecule on the cells,

making some of these observations due to chemical, not topographical, cues. The subject of patterned physico-chemical properties on substrates is another avenue of controlling directional growth and migration of cells which will not be discussed here (Ito, 1999). An *in vitro* study of DRG explants cultured at the ends of polypropylene multifilament bundles with varied diameters showed that filaments with 5 and 30 μm diameters had greater neurite extension and SchC migration than larger diameters of 100, 200, and 500 μm , a difference which was amplified when filaments were coated with FN, and even more so with LN (Wen and Tresco, 2006).

Thus far there have been no *in vivo* comparisons of topographical features and sizes, but the small nuances in feature size influences found *in vitro* with single cell cultures could well be lost when transferred to *in vivo* studies. In the experiments detailed in this dissertation the focus was on macro-scale architecture. Thus micro-scale topography was generally fixed and justified based on the *in vitro* studies outlined above. When micro-scale grooves (microgrooves) were incorporated into scaffolds, they were uniformly in the range of 30-50 μm with V-shaped profile, thus the grooves and ridges were of tapered width. The tapering could be considered a compromise between the various size limits ranging from single to tens of microns. The orientation with respect to different axes is the only aspect varied between experimental groups, and details of these can be found in each chapter.

2.2.4 Mechanical properties and neural cell behavior

Aside from the topographical properties, materials also have mechanical properties which are important in all tissue types from bone to brain. Much work is focused on hydrogels because of their comparable mechanical properties to the bulk properties of the nervous system, soft. There are several very specific measurements of different moduli (shear (Darvish and Crandall, 2001), tangent (Fallenstein et al.,

1969), compressive (Miller and Chinzei, 1997)) and permeabilities (Linninger et al., 2007) for different parts of the nervous system (white matter, gray matter (Coats and Margulies, 2006; Prange and Margulies, 2002), pia mater (Aimedieu and Grebe, 2004), spinal cord (Fiford and Bilston, 2005), brain (Miller and Chinzei, 2002)) mostly intended for finite element analysis and models for surgical planning. However, developing materials with this level of detail can be quite challenging, and the need for exact matching is unknown. Some studies have shown improved neurite extension in softer collagen gels than stiffer (Willits and Skornia, 2004). Another study shows neurons behave similarly in all stiffnesses of polyacrilamide or fibrin gels yet astrocytes attach, spread, and organize their cytoskeleton better on stiffer materials (Georges et al., 2006). They contend that use of a softer gel would increase the ratio of neurons to astrocytes in a regenerating population. However, it is also possible to design composite implants with a soft hydrogel embedded within a relatively stiffer scaffolding which could enhance astrocytic infiltration to provide its natural matrix support while allowing neurons to grow within the hydrogel in the matrix. This is a future application envisioned with the macro-architectural design hypothesis of this dissertation.

Various scaffold types have been investigated for CNS repair, mostly related to SCI. Though they fall within current strategies for CNS repair they will be discussed in the next section on macro-scale architectural influences and how they relate to the problem statement for this dissertation.

2.3 Macro-scale architectural influences and potential uses

We know on a cellular scale that topological cues and chemical and molecular cues are important and can influence cell survival, growth, and phenotype. The general

hypothesis for this dissertation is that architecture on a larger scale can affect tissue growth in the CNS. When one is no longer *in vitro* but rather *in vivo*, the system of evaluation is the whole tissue. If the architecture of a scaffold on its own is able to improve the regeneration potential in the CNS, its use would enhance the effects of other combination treatments like neurotrophic factors or implanted cells. Use of appropriate architectures could also potentially decrease any dosing requirements for expensive or limited treatments such as recombinant proteins or autologous cells. It is thus hypothesized that creating a more diverse set of macro-architectures based on known anatomical characteristics of the tissue would improve the regenerative capacity of the CNS.

This architectural question is easily discussed for skin, which has an obvious aspect ratio for its regeneration, and vasculature which is tubular. Bone has a need for porosity to encourage ingrowth, while providing mechanical support. One might argue that the tube or cylinder is already the obvious anatomical shape for the spinal cord but other architectures have not been investigated though a cylindrical scaffold with detailed channels for specific fiber tracts has been proposed (Friedman et al., 2002). The majority of regenerative work in nervous tissue began in peripheral nerve repair, as its propensity to regenerate is greater, and its natural architecture is similar to vasculature: tubular, with a longer aspect ratio than the spinal cord. The use of guidance tubes in SCI studies is no doubt a translation from its use in peripheral nerve repair studies. The brain has no history of this type of discussion, and is admittedly more difficult than the spinal cord as its organization and fiber tracts are so complex and varied. The following subsection is a review of materials and macro-architecture recently applied to CNS regeneration and their benefits and pitfalls. Because there are so many examples of materials fabrication with the intent

of SCI repair, the following summary will include only those with accompanying *in vitro* or *in vivo* study with neural cells or tissues, and focussing mainly on *in vivo* studies. Fabrication techniques for materials will not be discussed in detail unless directly relevant to the work done for this dissertation.

2.3.1 Scaffolds for brain injury repair

Most studies of biomaterials for use in brain trauma involve the use of hydrogels which can be injected into a cavity and take on the shape and size *in situ* with no pre-designed macro-architecture. Hyaluronic acid hydrogels have been investigated with some neural adhesive functionalization such as LN (Hou et al., 2005) or poly-D-lysine (Tian et al., 2005a) and improve cellular infiltration, neural tissue integration, and neurite extension into the gel compared to the gel without modification. Collagen gels, which alone do not support regeneration, when mixed with FN aid in neural stem cell (NSC) survival when injected into injury cavities (Tate et al., 2002). Another hydrogel, methyl-cellulose, injected alone into rat brain is biocompatible in the brain, though it gives no benefit either (Tate et al., 2001). A non-degradable hydrogel, poly N-2-hydroxypropyl-methacrylamide (pHPMA), functionalized with a peptide sequence for the adhesive and neurite promoting region of LN, improves the angiogenesis and axonal growth into this hydrogel *in vivo* (Cui et al., 2003).

Aside from injectable hydrogels, synthetic degradable implants have also been implanted. A woven mesh of poly(glycolic acid) (PGA) fibers of 10-15 μm diameters was used to culture NSCs *in vitro*. The architecture was random with micro-scale features from the fibers. This material and cellular composite was implanted into the injury cavity of rats after a hypoxic ischemic event (Park et al., 2002). The implant was able to support tissue integration and improvement of neurological function, and reduced secondary damage, mostly attributable to the presence of NSC. PGA is a

quickly degrading member of a family of polyesters (poly- α -hydroxy acids) commonly used in tissue engineering applications. An *in vitro* study of the biocompatibility of three related polymers, poly(lactic-co-glycolic acid) (PLGA, 75:25), poly(L-lactide-co- ϵ -caprolactone) (PLCL), and poly(L-lactide acid) (PLLA) on NSC determined that, of the three studied, PLGA supported greater viability, neuronal differentiation, metabolic activity, and less apoptotic activity. PLGA and its related polymers have been used in SCI applications as well and will be discussed in the next subsection.

No studies have been conducted on macro-scale architectural effects on brain tissue repair *in vivo*. Indeed, hydrogels are often unable to maintain macro-architectures, or they would need a higher concentration resulting in a higher stiffness and lower diffusivity. A scaffold similar to the mesh fibers just discussed could also be impregnated with a hydrogel, yet hold the entire composite within a macro-architecture. Because of the need to maintain an architecture, these types of implants could not be injected through minimally invasive techniques. However, in some cases of brain injury, craniotomy is used for reducing intracranial pressure, evacuating hematomas, or due to severe trauma the cranium is already damaged and should be removed from the interior cavity. In these cases an implantable scaffold might be a useful method of treating the injury, rather than an injectable hydrogel, since the cranium is already open and one can keep a scaffold spatially localized better than a semi-fluid hydrogel.

2.3.2 Scaffolds for spinal cord injury repair

There are several reviews of biomaterial strategies in spinal cord injury (Novikova et al., 2003; Zhang et al., 2005; Karp et al., 2003; Friedman et al., 2002; Hadlock and Sundback, 2006; Nomura et al., 2006). Because of the focus of this dissertation, the use of materials which cannot be formed into specific macro-architectures will be left

out of the background discussion for SCI. Hydrogels such as fibrin, collagen, agarose, hyaluronic acid, and Matrigel, which have been used in their hydrated gel-like state for injection or as a surgical implant with no other form of overall architecture will not be discussed. If they have been additionally processed to impart greater structure, such as freeze drying or used in conjunction with another material as a composite implant, they will be included here. Aside from gels, general architectures of note can be grouped into the following categories: random pored cylinder, tubes, multichanneled cylinders, and multifilament bundles. A poly(D-L-lactic acid)(PLA) and solvent mixture was freeze-dried to form a very porous foam whose pores were unidirectionally oriented and ranged in size from roughly 10 to 150 μm . This foam was cut into a cylindrical rod 4mm long and 2.6 mm in diameter and filled with a fibrin gel. In a transection model in rat, these foam cylinders did not support axonal growth into them. Adding BDNF by embedding with fibrin gel, axonal growth was marginally increased (Patist et al., 2004). These same cylinders, seeded with SchC which were transduced to secrete a BDNF/NT-3 multifunctional protein, had low cell survival and there was no difference in functional improvement with or without cells or polymer cylinder implant. A cylinder of randomly spaced oriented porous material was not beneficial, nor did it support survival of implanted cells (Hurtado et al., 2006). This PLA material was also then used to make porous tubes instead of cylinders, then filled with SchC. These implants were able to support small cables of regenerating neural tissue but collapsed after a few weeks, breaking into pieces and disrupting the tissue (Oudega et al., 2001).

In a similar freeze-drying method to the PLA cylinders (Patist et al., 2004), agarose gel was freeze-dried with dissolvable filament bundles interspersed to create a multichannel scaffold with additional isotropically oriented porosity in the bulk of

the material. This channelled agarose scaffold was used in a C4 hemisection model with recombinant BDNF (Stokols and Tuszynski, 2006), or BMSC transduced to express BDNF (Stokols et al., 2006). In part due to the hemisection rather than transection model, there was very linear axonal regeneration through these channels, additionally enhanced by the biological factors incorporated.

A non-degradable material, poly-acrylonitrile-poly-vinylchloride (PAN-PVC), was used to make tubes 8mm long and 3 mm diameter. These were also filled with Matrigel seeded with SchC. These scaffolds were cultured *in vitro* with SchC embedded in Matrigel until a bridge of aligned cells was formed. The distal end of the tube was capped, and after implantation at a T8 transection there was propriospinal axonal regeneration after one month into the tube from the proximal end (Xu et al., 1995b) which was improved with inclusion of BDNF and NT-3 (Xu et al., 1995a), and also with the administration of methylprednisolone at the time of surgery (Chen et al., 1996). When the distal end was uncapped and both ends of the tube were open, axons grew into both ends of the tube after one month, but the entering axons did not exit on the distal end into the stump (Xu et al., 1997). These tubes were then made smaller, 3 mm long and 1.25 mm diameter, with SchC bridges. They were placed in a hemisection model, rather than entubulating a complete transection model. Greater ingrowth and integration with the spared host tissue was seen and axons entered and exited the tube to form a continuous connection across the hemisection (Xu et al., 1999). The larger complete transection scaffolds were then implanted for three months and evoked potentials were generated in two out of nine animals, stimulating from within the scaffold and measuring 1 cm distal in the defect (Pinzon et al., 2001). Control tubes with just Matrigel and no cells did not generate any evoked potentials or support axonal regeneration in any of these studies. In all these studies, SchC or

neurotrophic factors were the main cause of any improvements.

Poly(lactic-co-glycolic acid) PLGA (85:15) was used in different fabrication technique to create a cylinder with 7 channels of 450 or 600 μm diameters. The walls of the channels were made porous from solvent evaporation (Moore et al., 2006). These scaffolds were seeded with SchC to induce axonal regeneration in a transection model as well. While they had no axonal regeneration within the scaffold without SchC implantation, they demonstrated an injection molding fabrication technique which could be modified to change the number and diameter of channels. Their scaffolds were designed for use as a template for the arrangement of cells to attract and guide axons. However, they also discussed the potential of very specific tubular designs incorporating individual shapes and sizes of different white matter tracts and building of a mold by free-form fabrication techniques, though a scaffold was not built from this mold, presumably because of the fine detail and delicacy of the mold (Friedman et al., 2002). Though these authors suggest that the locations of cells would be important, thus varying the scaffold architecture for reasons of placement of cells would be important, they do not suggest that the architecture of the material itself would have an effect on nervous tissue regeneration.

Poly(2-hydroxyethyl methacrylate-co-methyl methacrylate) (pHEMA-MMA) is a non-degradable material used for contact lenses. It is a hydrogel able to maintain its architecture. It is the subject of several studies in SCI. Tubes with two different elastic moduli (177 kPa and 311 kPa) were made of this material and implanted in a complete transection without any filler or biological cues. Axonal regeneration was seen within these tubes, and to a greater extent in the 311 kPa tubes (Tsai et al., 2004), in contrast to other studies with different materials previously discussed where no regeneration occurred unless SchC or neurotrophic factors were

incorporated. Though the pHEMA-MMA tubes may have had a slightly smaller gap between transected stumps, this study highlights the potential benefits of material and architectural designs prior to addition of biological factors. These tubes were then studied with different hydrogel matrices (collagen, fibrin, Matrigel) and neurotrophic factors (FGF-1, NT-3) as well as 4 smaller tubes within the larger channel (tubes within channels, TWC) to create a channeled scaffold with greater surface area. The TWC improved functional recovery over the empty single tube, and also over some of the other groups containing matrix and neurotrophic factors (Tsai et al., 2006). Some vestibular and reticular brainstem motoneurons were also found regenerating within the TWC. This study also calls attention to the possibility of different types of matrices to encourage regeneration of different types of axons and neurons. What is most interesting in these studies is the affect of TWC compared to an empty tube. The changing of the scaffold architecture, and thus surface area, affected the regeneration and functional recovery to a measurable extent.

However, the authors later mention that some of their tubes collapsed during the experiments (Nomura et al., 2006), an event also documented with the previously discussed PLA tubes (Oudega et al., 2001). They then reinforced those tubes with denser coils of the same material, but did not continue study of the TWC. Instead they placed these reinforced pHEMA-MMA tubes in a spinal cord transection with and without a peripheral nerve graft and FGF-1 incorporated inside the tube (Nomura et al., 2006). The addition of SchC and FGF-1 did not improve results compared to the empty reinforced tube, and additionally the results for these tubes were worse than previous non-reinforced implants. This is in contrast to the many studies already discussed where SchC and neurotrophic factors significantly improved outcomes with other material scaffolds. Entubulation methods involve placing the

stump ends inside the tube scaffold. They note that possibly the tubes were too small, pinching the stumps and causing syringomyelia and caudal migration of the rostral stump. This difference in results suggests that architecture could be quite important in the regenerative and reparative conditions, and the effectiveness of biologics.

Of the scaffold types discussed for SCI, the random pored cylinder and smaller tube for hemisection, and multichannel cylinders do not involve potential constriction of transected stumps as entubulation methods do. Another scaffold type which is non-constricting and also incorporates micro-scale linear topographical cues is the multi-filament bundle.

Cylindrical bundles of 10,000 $5\mu\text{m}$ diameter carbon filaments were implanted in 5mm long spinal cord transections and shown to integrate into the spinal cord tissue and support axonal guidance (Khan et al., 1991). These filaments were within the range of feature sizes described to align neurons *in vitro* as described in the previous section. More recently, 4000 collagen type I filaments of $20\mu\text{m}$ diameter were bundled and implanted in 5mm defects and were able to integrate into the tissue and improve functional outcomes as measured by BBB scores (Yoshii et al., 2003). Furthermore, these researchers compared those longitudinally aligned bundles to bundles of collagen fibers aligned perpendicular to the rostro-caudal axis and found poor recovery and integration (Yoshii et al., 2004), indicating the longitudinal alignment of micro-scale features to be important *in vivo*. However, they did not vary the macro-architecture, using only a bundled geometry within a tube.

2.3.3 Designed architectures in the central nervous system

Some researchers have already agreed that designed architectures can be used as tools in CNS regeneration, specifically for spatially localizing specific cells (Moore et al., 2006; Friedman et al., 2002) or different tubes containing different neurotrophic

factors (Tsai et al., 2006). Topographical cues could be strategically placed to aid in axonal guidance. Insightful architectural design could provide structural support from collapse while impeding scar tissue impingement and preserving a region for regeneration and vascularization. There are many conformations which can be imagined for CNS repair. The main obstacle is often fabrication techniques.

Fabrication methods: One method developed for fabrication of designed scaffolds in tissue engineering has been solid free-form fabrication (SFF) (Hutmacher et al., 2004). A wide variety of 3-D designs can be made with various computer software, including Rhinoceros (McNeel North America, Seattle, WA). Different SFF techniques exist: selective laser sintering, sterolithography, 3-D wax printing. Scaffolds can be made directly or indirectly through molds built by SFF techniques (Hollister, 2005). A 3-dimensional object file is generated which can be separated into a stack of 2-dimensional layers with an intended nominal thickness. With a 3-D printer, each 2-D layer is printed on a stage in a wax-like material to generate a raised 2-D cross-section of the 3-D object. Each layer is printed on top of the next as the stage lowers the printing surface by the layer thickness and trims the previously printed layer to the appropriate thickness. Through this layer-by-layer printing method, features as low as 250-300 μm can be created with great accuracy. Additionally, at the object's surfaces a groove is created between each layer which is the size of the layer thickness printed. Orientation of these aligned grooves on the object surfaces can be changed by changing the orientation of the object as it is built.

With the information on the importance of topographical cues and intrinsic anatomical structure and the capabilities for detailed fabrication from SFF techniques, a wider range of architectures can be investigated.

Designed scaffolds made for the work presented in this dissertation were made in molds built on a 3-D printer. A salt leaching technique was used (Mikos et al., 1994) to cast a porous polymer into the mold. Poly(ϵ -caprolactone) was used in all designed scaffolds so that the scaffolds would be porous and strong, yet soft and compressible. Between 65-85% porosity, the compressive strength of salt leached PCL is on the order of 100-250 kPa and the compressive modulus 500-1000 kPa (Olah et al., 2006). Details of fabrication will be described in the following chapters. Briefly, molds were designed in Rhino and built on a 3-D wax printer. Molds were packed with size-sieved salt crystals prior to polymer casting to ensure interconnection of the salt crystals and therefore pores. If salt is mixed with the polymer solution, salt crystals can potentially become encapsulated in polymer. Polymer was dissolved in warm acetone and poured into the salt-packed molds. Acetone was allowed to evaporate overnight and wax mold was dissolved in BioAct solvent, then salt and BioAct were removed with several washes of 70% ethanol.

Anatomically inspired designs: The organization of the central nervous system varies from location to location, thus to begin designing architectures based anatomical organization one must first choose locations. The cerebral cortex and thoracic spinal cord of rat have undergone investigation in the past with focus on traumatic brain and spinal cord injuries and are chosen here to continue in that vein.

The organization of the cerebral cortex, a gray matter region, is conserved quite well over the vertebrate species. (Figure 2.1) The mature thickness is generally a few millimeters, 3-4 in humans, 2-3 in rodents. The thickness can be subdivided into six transverse or horizontal layers which contain different subsets and combinations of neurons. They can be broadly categorized as projection neurons or local interneurons. Though the layers are not physically separated, there are pathways

that connect specific layers to other regions of the cortex and also to deeper regions of the brain like the thalamus. Additionally, neurons connect horizontally with each other in small bundles to communicate (Kandel et al., 2000)(pp. 327-331).

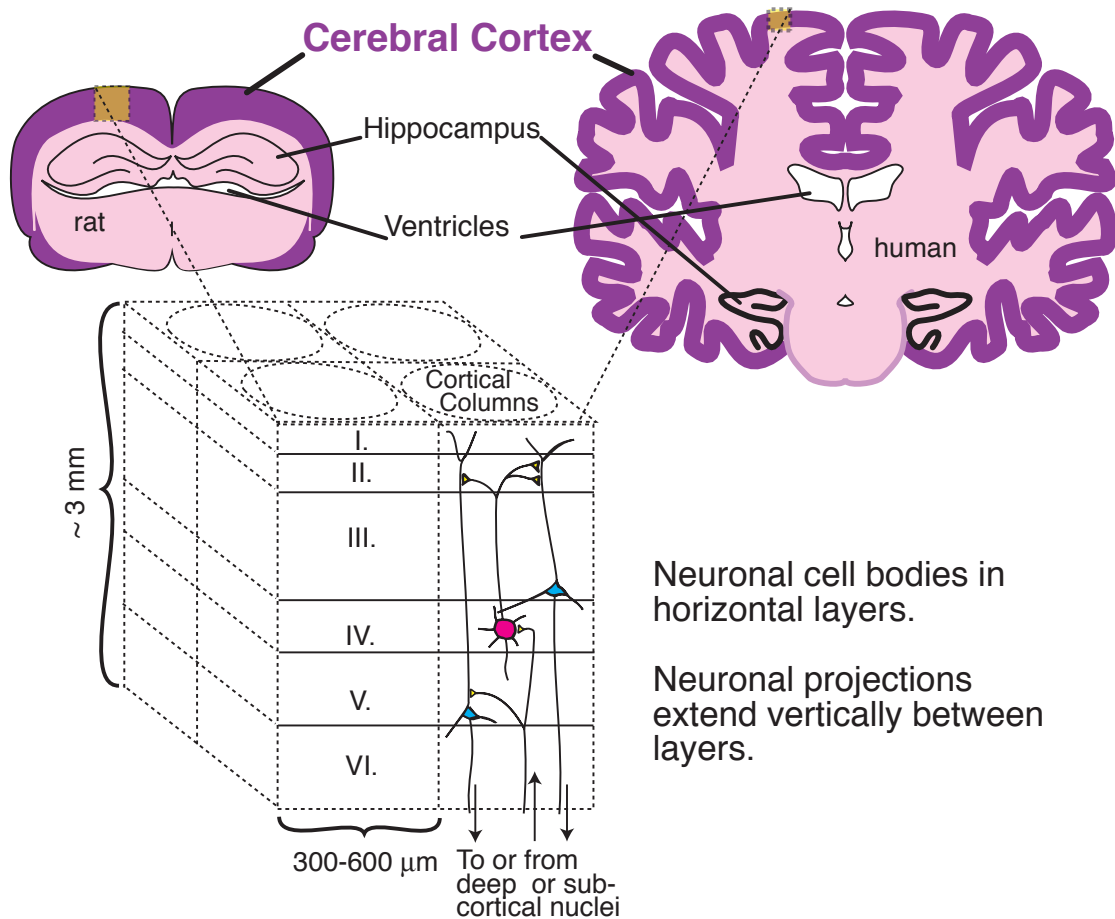


Figure 2.1: A schematic diagram of rat and human brain in coronal cross-section with cerebral cortex organization highlighted. Not to scale, the cerebral cortex (dark purple) in rat and human are roughly the same thickness. Due to the increased surface area of the human brain, there are more cortical columns, bundles of neurons forming a unit for processing information (dashed boxes), even though the size of individual columns is the same between species. The layers within the columns contain different types of neurons or the dendrites or axons and synapses from cells of other layers or parts of the brain. Axons project vertically, perpendicular to the pial surface, while the different cell layers are oriented horizontally.

Functionally, the cortical neurons are organized and communicate in bundles called cortical columns (Figure 2.1). These columns run vertically, perpendicular to the surface of the cortex or the pial surface depending on the presence of wrin-

kles. Neurons in these columns extend their axons and dendrites vertically to connect with each other from layer to layer across all six layers and also horizontally for much shorter distances to communicate within the column. The diameters of these columns are 300-600 μm in diameter, a size also conserved across species (Mountcastle, 1997). Evolutionary expansion of the cortex is accomplished through increasing the surface area through the number of cortical columns, not the size of the individual columns. Thus a primate or human can have a cerebral cortex much like rodents, made up of the same sized columns and roughly the same thickness of cortex, but with large gyri and sulci and a greater volume to cover. Rats have a fairly smooth cortex, not wrinkled like humans. Since the cortical neurons are organized in two ways, 1) horizontal layers of specific neuronal cell types and long distance communication and 2) vertical cortical columns of local communication and axonal projections, these linear and orthogonal directions could be imitated in designed architectures. These structures are incorporated into work for this dissertation on brain regeneration by creating channels of 300 to 500 μm in diameter oriented both vertically and transversely, and microgrooves of roughly 30-40 μm scale oriented in both directions.

The thoracic spinal cord contains both gray and white matter. In cross-section the gray matter, located in the center, has a characteristic butterfly or H shape and contains the cell bodies of mainly sensory neurons, motor neurons, and interneurons (Figure 2.2). The ventral horn of the gray matter contains motor nuclei whose axons project through the ventral roots to innervate skeletal muscles. The dorsal horn contains sensory neurons which convey sensory information from dorsal root ganglion sensory nuclei to the brain. Interneurons play a variety of roles in communication between the brain and sensory and motor neurons or between motor neuron groups in the spinal cord. Typically in a spinal cord injury the gray matter dies first, followed

by the white matter (Schwab et al., 2006).

Surrounding the gray matter is the white matter which is divided generally into dorsal, lateral, and ventral columns. The ascending and descending axonal pathways are located in the white matter and can be subdivided into specific tracts connected to specific parts of the brain and brain stem (Figure 2.2). When ascending or descending axons reach appropriate segments of the spinal cord they branch inward to the gray matter to connect with specific neurons. Propriospinal neurons are located medially in the gray matter of the spinal cord and their axons can run up and down the length of the spinal cord in the medial and ventral regions of the white matter, called propriospinal tracts, to connect areas of the spinal cord for axial muscle control such as postural adjustment, or reach shorter distances to coordinate more distal limb functions. Descending tracts from the brain stem are subdivided into two systems, the medial and lateral. Medial pathways from the brain stem, (vestibulospinal, reticulospinal, and tectospinal tracts) connect with ventro-medially located interneurons and propriospinal neurons in the grey matter, thus serving in the control of axial and proximal muscles, like posture control and core muscles. These descending brain stem tracts are found mainly in the lateral and ventro-medial columns of the white matter. Lateral pathways from the brain stem descend mainly in the rubrospinal tract from the midbrain and follow the dorso-lateral regions of the white matter. This tract helps to control limb movements such as reaching and manipulating. Another source of descending axons in the spinal cord is the cerebral cortex, most notably the motor cortex and are known as corticospinal fibers and tracts. Some nerve fibers from the cortex, corticobulbar fibers, terminate at the brain stem and indirectly continue through the descending tracts of the brain stem. There are also two corticospinal tracts, which descend all the way through the spinal cord in the

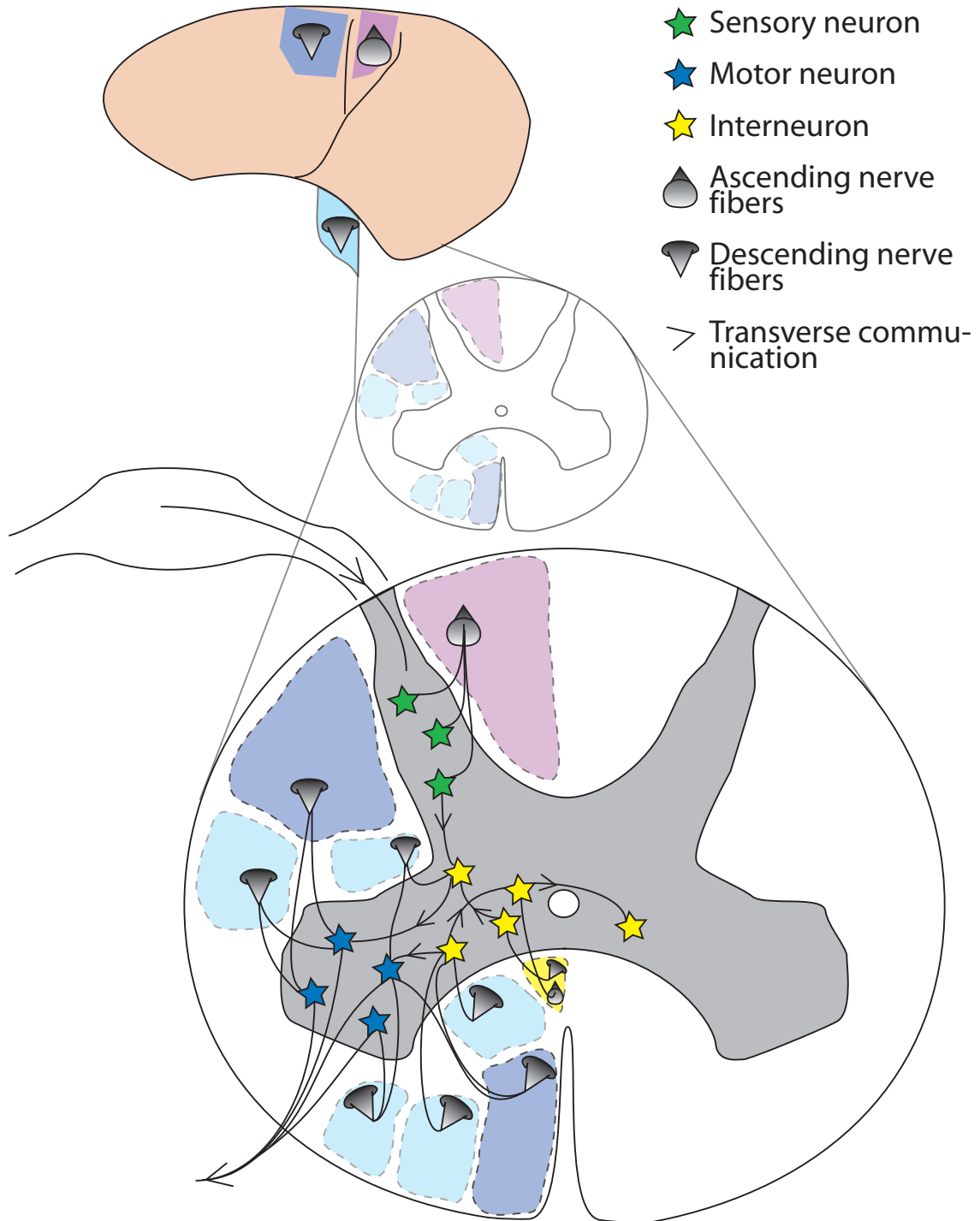


Figure 2.2: A schematic diagram of the spinal cord. The cord is generally symmetric across the midline. Ascending nerve fibers from the sensory neurons (green stars) project through the dorsal column (pink) of the white matter. Descending fiber tracts from the motor cortex (dark blue) and brain stem (light blue) descend in the lateral and ventral regions of the white matter to connect to the motor neurons (blue stars) and interneurons (yellow stars). Propriospinal neurons are interneurons which can connect motor and sensory neurons between different segments of the spinal cord by projecting through a ventro-medial tract (yellow) of the white matter. This diagram highlights the circumferential location of fiber tracts and the central location of neurons and transverse communications between those neurons.

ventral and lateral white matter columns. The lateral corticospinal tract connects largely to motor neurons in the lateral ventral horn and interneurons slightly medial for control of limb movements. The ventral corticospinal tract controls more axial muscles by connecting to more medial motor neurons on both sides of the spinal cord in the ventral horn. Ascending axonal tracts are found largely in the dorsal column, which carry the somatic sensory information to the brain stem. Ascending sensory axons in the lateral and ventral columns carry pain and thermal sensations. (Kandel et al., 2000)

The organization of the spinal cord can be simplified to circumferentially located longitudinal fiber tracts surrounding and intermittently connected to a core of intermingled cell bodies. The longitudinal tracts and central core delineations could be replicated in designed architectures. The designs created for spinal cord regeneration based on these architectural features are described in detail in Chapter 5.

CHAPTER III

PCL and PLGA degradable polymer sponges attenuate glial scarring and lesion growth in traumatic brain injury

3.1 Overview

This study evaluated the response of rat cerebral cortex to two degradable polymers, poly-(L-lactic-co-glycolic acid) (PLGA), and poly(ϵ -caprolactone) (PCL), two common materials in tissue engineering. PLGA has been extensively studied in the brain for controlled drug release as injectable microspheres, and is generally accepted as biocompatible in that capacity. Biocompatibility in other forms and for different functions in the brain has not been widely studied. PCL was chosen as an alternative to PLGA for its slower degradation and less acidic pH upon degradation. Porous scaffolds were made from both polymers and implanted into rat cerebral cortex for 1 and 4 weeks. Morphology, defect size, activation of microglia (OX-42) and astrocytes (GFAP), infiltration of activated macrophages (MHC-II), and ingrowth of neurons (Tuj1) and progenitor cells (nestin) were analyzed by H&E staining and immunofluorescence. PCL induced a lower inflammatory response than PLGA as demonstrated by lower MHC-II and GFAP expression, and greater ingrowth. Both polymers alleviated astrocytic activation and prevented enlargement of the defect when compared to an empty defect. Tuj-1, nestin, and GFAP positive cells were observed growing on both polymers at peripheries of the sponge implants, demonstrating their permissive-

ness to neural ingrowth. These findings suggest both polymers attenuate secondary death and scarring, and that PCL might have advantages over PLGA.

3.2 Introduction

Brain lesions can result from a range of causes, from traumatic injury to disease. The resultant voids are unable to retain or support injections of suspension treatments such as cells or growth factors, which disperse quickly and lose effectiveness. From a tissue engineering stand point, a delivery vehicle which fills the void and contains drugs, neurotrophic factors, or cells has the potential to localize and maintain these treatments in the implant site, increasing the effectiveness, and provide a path toward repair and reconstitution of the lost parenchyma which is lacking in current clinical treatments (Thompson et al., 1999). This delivery vehicle must satisfy certain design criteria, such as permissiveness to neural cell growth and immunological compatibility. Such scaffolds should not cause significant inflammatory responses that may exacerbate the injury. Also mechanically the material must be close enough to the tissue dynamics that surgical insertion and normal movements of the patient do not cause more physical damage.

Treatment strategies for brain injuries such as hypoxic ischemia models focus mainly on combination treatments using cells or neurotrophic factors (Park et al., 2002; Tate et al., 2001; Tian et al., 2005a). Studies focusing on combination treatments often overlook the potential importance of the material itself, and often compare improvements and outcomes to a completely empty control site rather than the untreated material. Different materials, such as gels and polymer fiber meshes, have been studied separately. Unfortunately, there are no good comparisons of materials, or any in-depth study of the relative biocompatibilities of the materials themselves.

To provide an optimal outcome, it would be important to study and determine the best combination of biologic therapy and material vehicles in a systematic approach.

PLGA and its related components are among the most widely investigated degradable polymers in biomedical applications. The most extensive work with PLGA regarding material-brain research has been in controlled drug release applications in the form of microspheres injected into brain (Fournier et al., 2003; Kou et al., 1997; Popovic and Brundin, 2006). PLGA has been generally accepted as biocompatible in that capacity. PCL has also been studied in the brain for controlled release microspheres (Fournier et al., 2003; Menei et al., 1994), though not as extensively as PLGA. PCL has been most commonly studied in other tissue types and has a history of drug delivery and tissue engineering research elsewhere in the body (Sun et al., 2006; Tang et al., 2004; Taylor et al., 1994). CNS inflammation has also been studied in the context of electrode implants, where close contact of neuronal activity is desired (Polikov et al., 2005). The current study investigated the biocompatibility of both PLGA and PCL in the capacity of CNS tissue engineering. This approach requires ingrowth and close contact with regenerating neuronal structures and integration of host tissue within and around the implant. The structure of a scaffold in a defect, rather than microspheres injected into tissue, may elicit a different host response. The definition of biocompatibility here is slightly different from controlled release and implantable electrodes, and we take guidance from both areas.

Acute inflammation in various brain injury models occurs over the course of hours to days, encompassing hemorrhage, degeneration of damaged neurons, and macrophage infiltration. By 7 days the inflammatory response has elicited secondary cell death mechanisms which result in degeneration of white matter and expansion of the original injury site. The ultimate size of the defect depends greatly on the

initial insult. Thus different CNS defects may require different standards for success. It may be useful in some cases with very large defects for the scaffold to have a much longer residence time and sturdier support than can be offered by most hydrogels and PLGA derivatives. PCL could fill this requirement. It is possible to use PCL as a scaffold to carry cells within a hydrogel which infuses its pores, giving the implant a definite structure and longer lasting support once the gel has dissipated and the cells are establishing a full matrix. Though the degradation rates of both PLGA and PCL can be adjusted through their initial molecular weights and the ratio of lactic acid to glycolic acid in the case of PLGA, PCL may offer another benefit in the lower acidity of its degradation product, caproic acid ($\text{pKa} = 4.84$) compared to lactic acid ($\text{pKa} = 3.08$) and glycolic acid ($\text{pKa} = 3.83$).

Both polymers degrade by hydrolysis of the polymer chains. The difference in their degradation rate is mostly a result of their differing hydrophobicities. PCL is more hydrophobic than PLGA and therefore is hydrolyzed more slowly than PLGA. As the molecular weight decreases, and polymer chains become smaller, macrophages phagocytose these small particles. Porous implants of PCL and PLGA in a subcutaneous site were reported at 4 weeks to have lost 39% and 74% of their molecular weights, respectively. Additionally, these researchers have shown PCL to have higher total cellular ingrowth than PLGA after 4 weeks, and higher inflammatory cell invasion and angiogenesis subcutaneously. This study compared PCL to PLGA in a salt-leached sponge architecture as they relate to brain inflammation and ingrowth in an injury site. We found that PCL elicited a lower immune response than PLGA and both polymers lowered the scarring and secondary cell death after injury compared to a defect without implant.

3.3 Methods

Porous scaffold fabrication

PCL (CAPA 6501, MW 50 kDa, Solvay Chemicals, Houston, TX) and PLGA (50:50, MW 54 kDa, Birmingham Polymers, Birmingham, AL) were used in this study. Both polymers were made into sponges by solvent casting and porogen leaching with 180-250 μm NaCl crystals in a Teflon mold to form 3mm diameter cylinders of 3mm height. PCL was dissolved in acetone and PLGA in chloroform at 13% (w:v) and dripped into salt packed molds from both ends until no more polymer could be absorbed. Scaffolds were sterilized in 70% ethanol and then switched to sterile Hanks Balanced Salt Solution and placed on a shaker one day prior to implantation. Prior to scaffold fabrication PCL was cast separately with two different solvents, acetone and chloroform to examine the microstructure and roughness under scanning electron microscopy (SEM). Chloroform was used with PLGA because it does not readily dissolve in acetone and it was necessary to maintain a comparable surface to the PLGA microspheres previously studied and deemed biocompatible for comparison with PCL.

Surgical implantation

Female Sprague-Dawley rats (250g) were anesthetized with isoflurane and heads were mounted in a stereotaxic device. The skulls were exposed, bregma located, and two positions marked, 3mm posterior and either 3.5 mm left or right. Holes were drilled in the skull with a 3mm outer diameter trefine at one or both locations. Bone chips were removed and then the same trefine, which had a marking 3mm from the bottom of its burr, was used to drill 3mm into the cerebral cortex. The drill was kept perpendicular to the surface of the skull and was held steady during the removal of

brain tissue by the hole in the skull. PCL and PLGA sponges were inserted into the right and left cavities, respectively. Controls received no implant in either cavity. Other researchers report the lack of contralateral damage and inflammation in a similar injury model (Chen et al., 2003). To confirm this in our own studies 7 rats received only one defect in either the left or right hemisphere. The distribution is described below. In the 1 week time point: 2 rats for control (no implant) both in the right hemisphere, 1 rat with PLGA in the left hemisphere. In the 4 week time point: 3 rats with PCL with one left and two right hemisphere implants, and 1 rat with PLGA in the left hemisphere. Tissue was examined histologically and with all the immunofluorescent inflammation markers used in the study. Once it was confirmed that the contralateral sides were not affected and there was no difference between the right and left hemispheres, these data were combined with data for rats containing 2 defects per brain for a total of 4 samples per group per time point. At 1 week and 4 weeks, rats were perfused transcardially with 250 mL of 4% paraformaldehyde in phosphate buffered saline. Brains were harvested and cryoprotected, then serially sectioned coronally at 14 μm thickness in groups of 5 for further analysis. There was no noticeable loss of motor function due to the surgeries and no noticeable difference between groups in functional behavior after the surgery. All surgery, post-surgical recovery and euthanasia were performed according to a protocol approved by the University of Michigan Committee on the Use and Care of Animals.

Immunofluorescence, staining, and microscopy

Immunofluorescence was carried out using MHC-II (MCA46GA Serotec, Raleigh, NC), nestin (Rat-401 Hybridoma Bank, University of Iowa), Tuj1 (MMS-435P Covance, Berkeley, CA), GFAP (G9269 Sigma), and CD11b(OX-42) (MCA275G Serotec) primary antibodies were used with either Cy-2 conjugated secondary antibody or

Streptavidin AlexaFluor-488 (Invitrogen/Molecular Probes, Carlsbad, CA) with VectaStain ABC kit and biotinylated secondary antibodies (Vector Labs, Burlingame, CA). Harris hematoxylin and alcoholic eosin stains were used for assessing a general overview of inflammation and morphology. Images were taken using a Spot camera and Spot Advanced software. All images for a montage were taken in the same sitting with the same exposure and processing settings. When possible, all images of sections with the same type of labeling were taken on the same day or two to three consecutive days in batches of 15 to 20 slides. Positive and negative control labeling was done with all primary and secondary antibodies using stock sections from undamaged rat brain to verify their specificity and check background staining. A mixture of 5% donkey serum (Jackson ImmunoResearch Laboratories Inc., Westgrove, PA) and 3% BSA was used for blocking non-specific binding.

Quantification and statistics

Pixel areas for MHC-II and intensities for GFAP and OX-42 antibodies were calculated using programs written in Matlab (Mathworks, Natick, MA) (program details see section 6.3). The programs were written to allow the user to define specific regions of interest and calculate mean grayscale values (between 0 and 255) to determine background intensity and experimental group intensities. All intensity data presented have background subtracted. Also, for MHC-II quantification images were thresholded to exclude background areas. Then paths were drawn in Adobe Photoshop to encompass total sponge area and used as a mask for the scaffold area to be thresholded. Debris and halos were removed with Photoshop prior to calculating areas based on intensity thresholds. GFAP and OX-42 intensities were calculated from two neighboring 200 μm wide rectangles along each side of each scaffold (Figure 3.1).

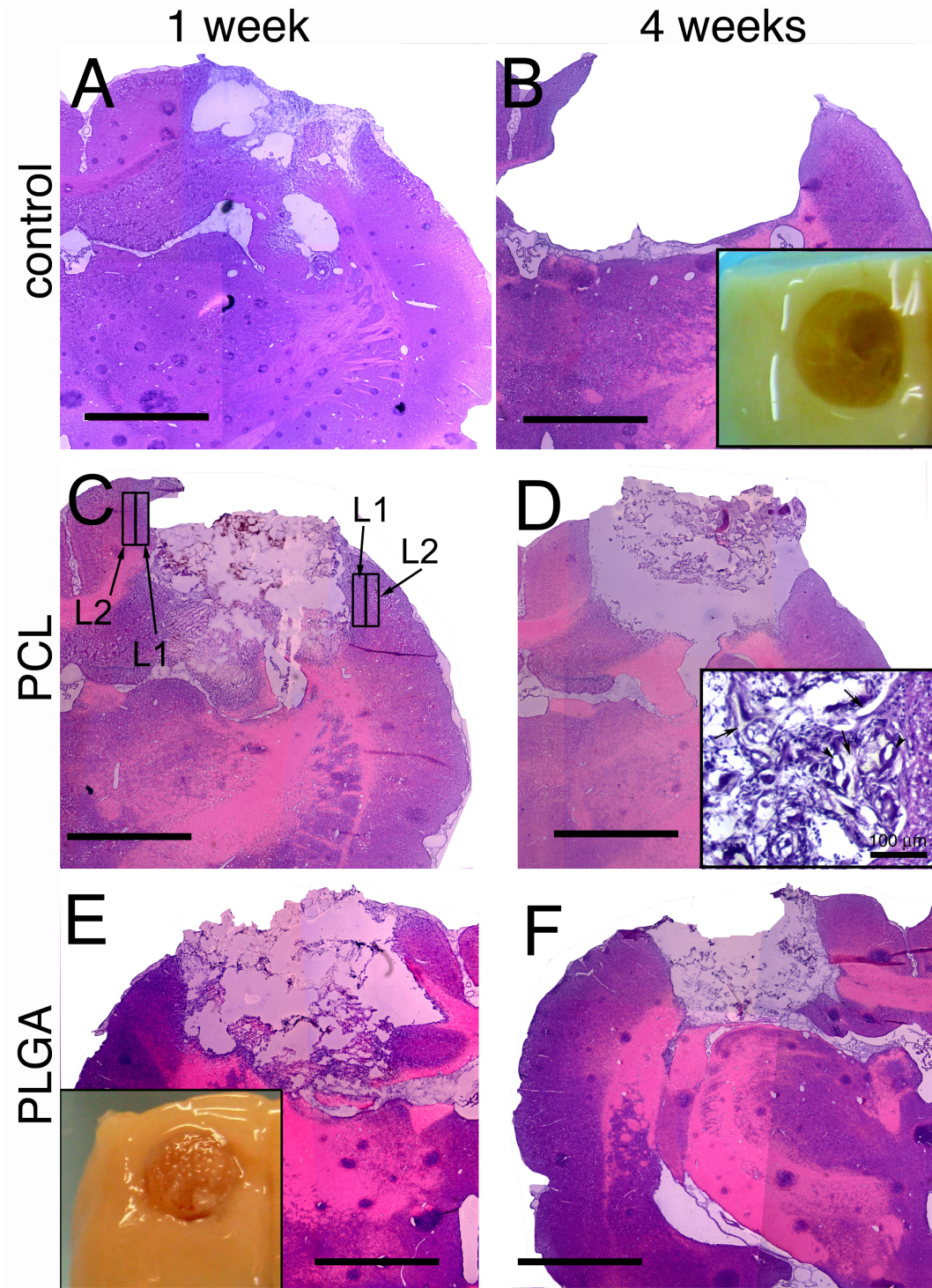


Figure 3.1: H&E stained sections of PCL and PLGA polymer constructs in brain cavities. (C) regions L1 and L2 are illustrated on this section. All images (except for insets) were taken at 2x magnification and tiled together. Scale bars are 2 mm unless otherwise labelled. Control at (A) 1 week and (B) 4 weeks, PCL at (C) 1 week and (D) 4 weeks, and PLGA at (E) 1 week and (F) 4 weeks. (inset B and inset E) Gross images before sectioning illustrate the visual difference between (B) control and (E) a defect containing material. (inset D) 10x mag of H&E section showing parenchyma at the bottom corner of a defect site on the right-hand side with PCL polymer (arrows) and blood vessels (arrow heads).

Region L1 was the region immediately adjacent to the defect and L2 was the region just adjacent to L1. Each sample section had two L1 regions and two L2 regions, which were combined for an average. Lengths varied and regions were chosen to exclude edge effect fluorescence, the hippocampus, dirt particles, air bubbles, and folds. Three regions on each section were chosen from areas of the cortex unaffected by the surgeries to calculate background intensities on each slide. The average total area used to calculate background was 0.09 mm^2 . Statistical significance was calculated using a 2-way ANOVA over time and material for MHC-II areas and defect widths and 3-way ANOVA for GFAP and OX-42 intensities over time, material, and region. P levels below 0.05 were considered statistically significant. Tukeys Least Significant Difference was used in post-hoc tests when ANOVA showed significance among groups. Error bars in graphs show standard deviation. Cellular areas within sponges were calculated from H&E stained sections since the polymers did not stain, while combined cellular and material areas were calculated from immunofluorescence images due to the polymers persistence on slides after aqueous processing and their low-level autofluorescence. Defect sizes were measured with the measuring tool in Adobe Photoshop. Serial sections were measured until the middle of the defect was found and that measurement was used. Distances were measured across the top and across the middle as parallel lines, perpendicular to the apparent angle of entry for the axis of the cylinder sponges.

3.4 Results

Polymer Morphology

Acetone was chosen as the solvent for PCL because of its relative ease and safety compared to chloroform. However, use of the two solvents results in two different surface roughnesses as seen under SEM (Figure 3.2). Use of acetone results in a

rougher surface with additional porosity compared to the relatively smooth surface which results from using chloroform. The surface directly contacting salt revealed that in addition to the salt-generated pores, smaller pores between the walls were present when using acetone as solvent. The increased surface roughness and porosity were additional motivating factors for using acetone as the solvent to potentially increase cell attachment and nutrient diffusion through the scaffolds.

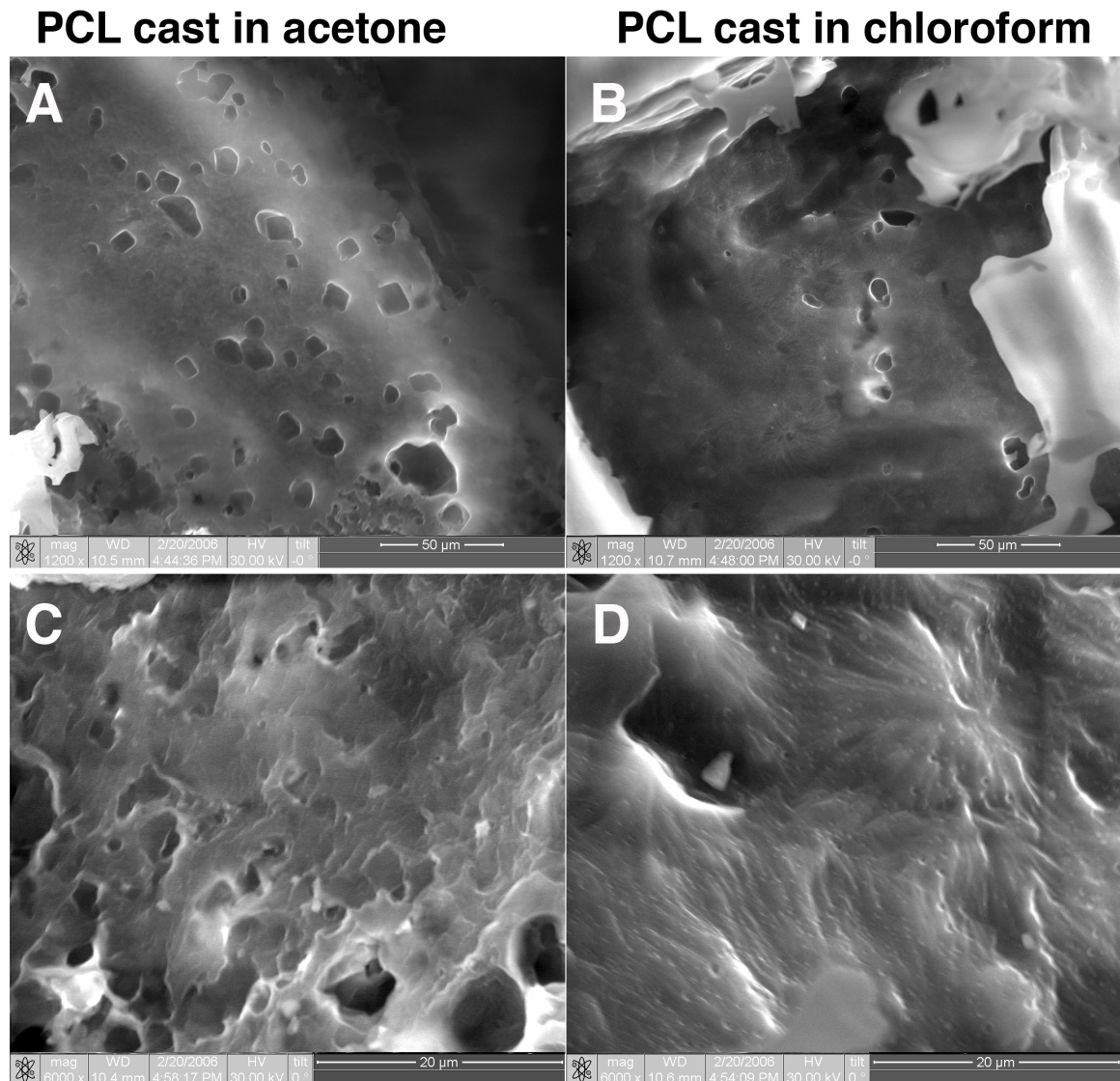


Figure 3.2: SEM micrographs of PCL surfaces cast with acetone and chloroform as solvents. The PCL surface which was in contact with a salt crystal has more pores when cast in (a) acetone than (b) chloroform. Scale bars in a,b 50 μm . The roughness of the surface on closer inspection is greater using (c) acetone than (d) chloroform. Scale bars c,d 20 μm .

Gross morphology

Defects in control brains without any polymer implant increased in size over the course of the experiment, whereas both PCL and PLGA helped to maintain the defect close to its original size. Brain tissue encompassed the sponges rather than shrinking away from it (Figure 3.1e inset). By measuring serial sections to find the middle of each scaffold, the defect widths revealed no significant difference between the two different polymers, but were significantly different from the controls. Both polymers were able to maintain the defect sizes at approximately the original size, while the control defect expanded to over 4 mm in diameter (Figure 3.1b inset and Figure 3.3a). From 2-way ANOVA over group and time only the interaction had significance, $P = 0.0194$. From the post-hoc analysis there was no difference between the two polymers at both time points. Only the control group was significantly larger than the materials at 4 weeks. At 4 weeks a noticeable difference in color and morphology appeared between PCL and PLGA sponges (Figure 3.1). After perfusion, PCL sponges were the same color as the surrounding brain tissue and PLGA sponges had a brownish red color that was consistent in all replicates. This may be a reflection of vascular connectivity within the sponges allowing blood to be perfused more thoroughly in PCL than PLGA sponges.

Coronal sections through the brains were used to observe the polymer sponge structure in the brain defect (Figure 3.1). Shapes reminiscent of salt crystals were evident. Groups at 1 week looked less empty, as fibrin clots remained. By 4 weeks clots cleared, but some peripheral tissue integration remained. Cells were seen in close contact with polymers and some vascularization was seen (Figure 3.1d inset). Additionally, at 4 weeks sponges began to degrade and had overall smaller volumes. In the H&E images, polymers were dissolved by the xylenes during staining, leaving

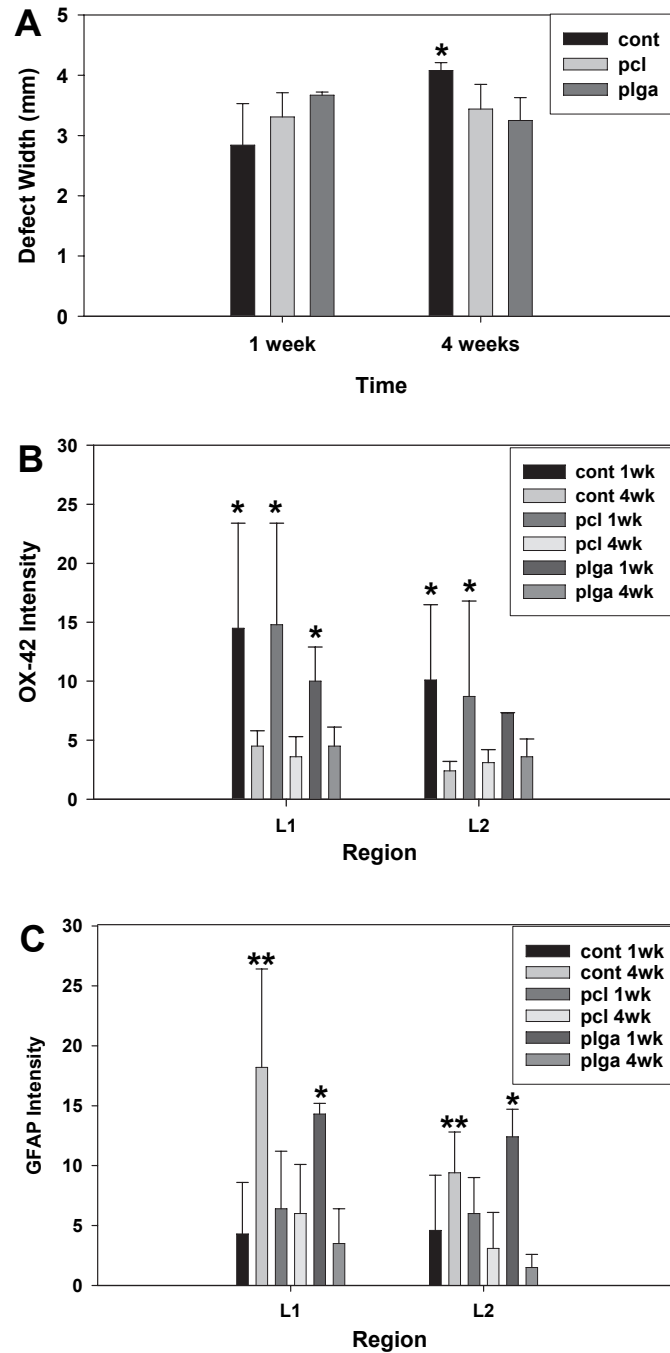


Figure 3.3: Quantitative data comparing control, PCL, and PLGA from image analysis. (A) Defect widths for each group at 1 and 4 weeks. Starred control is significantly larger than all other groups and times ($P < 0.05$). (B) Ox-42 intensities after background subtraction. Starred groups were not different from each other, but significantly higher than the unstarred groups. Unstarred groups were not significantly different from each other. (C) GFAP intensities after background subtraction. All starred groups are higher than unstarred groups. The two doubly starred groups are significantly different from each other. Unstarred groups are not significantly different from each other. (see text for detailed P values)